measured by mixing the medium with 50 μL of substrate mixture (20 U/mL GlDH, 2.5 mg/mL β-NAD, 0.25 mg/mL MTT, 100 μM MPMS, and 0.1% (vol/vol) Triton X-100 in 0.2 M Tris–HCl buffer (pH 8.2)) and incubating the mixture at 37°C for 30 min. The reaction was stopped by adding 100 μL of stop solution (50% (vol/vol) dimethylformamide and 20% (wt/vol) sodium dodecyl sulfate (SDS) in water (pH 4.7)). The amount of the reaction product (MTT formazan) was determined by measuring the absorbance at 570 nm (test wavelength) and 655 nm (reference wavelength) with a microplate reader. The extracellular L-Glu concentration was estimated from a standard curve, which was constructed for each assay using cell-free medium containing known concentrations of L-Glu. When the L-Glu was not applied after washing with fresh medium, no changes in extracellular L-Glu concentrations were observed in the 30 min incubation period in any experiments in this study. To measure the L-Glu released from microglia, the extracellular concentration of L-Glu was measured after 24 h of LPS treatment. The control values were almost same in the same culture batch but variable among different batches (40 to 60 μM). We therefore confirmed the reproducibility of the results in three independent experiments using different culture batches.

LDH and MTT assays

The lactate dehydrogenase (LDH) activity in the medium was evaluated according to a previously described method [33]. Briefly, 50 μL of culture medium from each well of a 96-well plate was mixed with 50 μL of substrate mixture (2.5 mg/mL lactate lithium salt, 2.5 mg/mL β-NAD, 0.25 mg/mL MTT, 100 μM MPMS, and 0.1% (vol/vol) Triton X-100 in 0.2 M Tris–HCl buffer (pH 8.2)). After a 10 min incubation at 37°C, the reaction was stopped by adding 100 μL of stop solution as described above. The amount of MTT formazan was determined using a microplate reader. The data were normalized to the averaged value of the group treated with 0.1% (vol/vol) Triton-X 100 for 1 h. MTT reductions were evaluated according to the manufacturer's instructions.

Real-time quantitative polymerase chain reaction (TaqMan RT-PCR)

The total cellular ribonucleic acid (RNA) was extracted from cells with an RNeasy Mini Kit and treated with RNase-free DNase to eliminate genomic deoxyribonucleic acid (DNA) contamination. The amount of total RNA was quantified by measuring the OD260 using a Nanodrop spectrophotometer (Nanodrop, Wilmington, DE). The reactions (25 μL) contained 1 ng of total RNA, 900 nM forward and reverse primers, 250 nM TaqMan probe, and RNase inhibitor mix in the master mix solution. The RT-PCR was performed using the TaqMan One-Step RT-PCR master mix reagent kit according to the manufacturer's protocol. The data were analyzed with 7,900 System SDS Software 2.2.2 (Applied Biosystems, Foster City, CA, USA) using the standard curve method. The GLAST and GLT-1 mRNA expression levels were normalized to the ribosomal RNA control (18S) expression levels. The primer sequences were as follows: 5'-GATCGG CATAATCATTGTCATCA-3', 5'-CGATTTTACCTTCTC TGTACATGTTTC-3' (GLAST), and 5'-CCGAGCTGGA CACCATTGA-3' 5'-AATGGACTGCGTCTTGGTCAT-3' (GLT-1). Specific probes for GLAST (TCCACCCCGG AAAGGGCACG) and GLT-1 (CAACACCGAATGAATG CACGAAGACATCGA) were used.

Western blotting

The cells were washed twice with PBS and once with lysate buffer (150 mM (wt/vol) NaCl, 10 mM (wt/vol) EDTA, 5 mM (wt/vol) EGTA, 0.5% mM (vol/vol) NP-40, and 0.5% (wt/vol) sodium deoxycholate in 10 mM Tris–HCl buffer (pH 7.4)). The protein concentration was measured using the BCA protein assay. The proteins (20 μg/lane) were mixed with SDS sample buffer (2% (wt/vol) SDS, 10% (vol/vol) glycerol, 0.25% (wt/vol) BPB, 5% (vol/vol) 2-mercaptoethanol in 125 mM Tris–HCl buffer (pH 6.8)), loaded onto a 10% polyacrylamide gel, electrophoresed, and transferred onto a PVDF membrane. The membrane was blocked with 5% (wt/vol) non-fat dry milk in Tris-buffered saline containing 0.1% (vol/vol) Tween 20. The membrane was incubated with rabbit anti-GLAST polyclonal antibody (1:4,000; ab65978, Abcam), mouse anti GLT-1 (1:2,000; sc-7760, Santa Cruz) or anti β-actin monoclonal antibody (1:5,000; A5316, Sigma-Aldrich) overnight at 4°C followed by incubation with the horseradish peroxidase-conjugated anti-rabbit antibody (1:20,000; Amersham Biosciences) or the anti-mouse or anti-goat antibody (1:20,000 Amersham Biosciences). The signals were scanned with an LAS3000 (Fuji Photo Film Co., Ltd., Tokyo, Japan) using an ECL western blot detection system (SuperSignal West Femto Trial Kit). For relative quantification of the expression levels of GLAST and GLT-1, we first compared the densities of the bands of the same amount of GLAST and GLT1 control proteins (full length) (1, 10 μg). In the LPS-exposure experiment, we normalized the band density of each subtype to the density of the 10 μg control band of the corresponding subtype. The bands of GLAST and GLT1 standard proteins were obtained at the same appropriate exposure time. The bands of GLAST and GLT1 in the LPS-exposure experiment were obtained at the same appropriate exposure time.

Immunocytochemistry

The cells were washed with PBS three times and fixed with 4% PFA for 60 min at room temperature. After

more washes with PBS, the cells were permeabilized and blocked for 60 min with 0.1% (vol/vol) Triton X-100, 5% (vol/vol) goat serum, and 1% (wt/vol) BSA in PBS. After washes with PBS, the cells were incubated with primary antibodies overnight at 4°C. Mouse monoclonal anti-Tuj1 antibody (1:500, MAB5564, Chemicon), chicken polyclonal anti-GFAP antibody (1:400, ab4674, Abcam), and rabbit polyclonal anti-Iba1 antibody (1:1,000, 019–19741, Wako) were used to stain neurons, astrocytes, and microglia, respectively. After washes with PBS, the cells were incubated with secondary antibodies (1:500, Invitrogen) conjugated to fluorochromes for 2 h at room temperature in the dark. After washes with PBS, fluorescent images of the cells were obtained by confocal microscopy (LSM5 Pascal, Zeiss).

Characterization of microglial releasing factors that downregulate L-Glu transporters

For the conditioned medium study, the astrocyte-microglia-neuron mixed culture was treated with LPS (10 ng/mL, 72 h), and the conditioned medium was transferred to the astrocyte culture. After 72 h, the L-Glu clearance assay was performed on the astrocyte culture. In a separate experiment, the astrocyte culture was incubated for 72 h with a transwell carrying microglia that had been treated with LPS, and the L-Glu clearance assay was performed in the astrocyte culture. For the serial applications of L-Glu, the medium of the astrocyte-microglia-neuron mixed cultures was replaced with fresh medium containing L-Glu (100 μM) every 2 h for 24 h. The L-Glu clearance assay, TaqMan RT-PCR, and western blotting were performed after the serial application of L-Glu.

The measurement of the astrocytic intracellular L-Glu concentration

The astrocyte-microglia co-culture was treated with LPS (10 ng/mL, 72 h) and washed twice with gentle shaking to remove microglia. After confirmation of the microglial removal under a microscope, 0.1% TritonX-100 was applied and incubated for 1 h. The L-Glu concentration in the supernatant was measured as described above. TBOA was applied from 1 h before the start of LPS treatment.

Statistical analysis

All data are expressed as the mean ± the S.E.M. Statistical analyses were performed with Student's t test or a one-way repeated-measures analysis of variance (ANOVA) followed by Tukey's post-hoc test for multiple pairwise comparisons, as shown in the figure legends. In all of the comparisons, the differences were considered statistically significant when P <0.05. All of the experiments were repeated in triplicate, and the same results were obtained in all of the sessions.

Results

L-Glu uptake was decreased during inflammation without cell death through the downregulation of GLAST expression

To definitively investigate the interactions between activated microglia and astrocytes, we used a mixed culture composed of astrocytes, microglia, and neurons. To quantify L-Glu transporter function, we measured the extracellular concentrations of L-Glu (that is, the concentration of L-Glu remaining) 30 min after a single exogenous application of L-Glu to the medium (the starting concentration was 100 μM). In this manner, we first determined the optimal conditions for inflammation without cell death. The cultures were treated with LPS for 72 h. The L-Glu remaining was significantly increased after incubation with 10 and 100 ng/mL LPS (Figure 1A). Significant LDH leakage and decreases in MTT reduction were induced by 100 ng/mL LPS but not by LPS concentrations less than 10 ng/mL (Figure 1B). In pure astrocyte cultures, significant decreases in MTT reduction were induced by 100 ng/mL LPS, but LPS concentrations less than 10 ng/mL did not affect either the LDH leakage or MTT reduction (Figure 1C). Whereas increases in MTT reduction were induced by 1 to 100 ng/mL LPS in pure microglial culture, significant LDH leakage was induced by 100 ng/mL but not by LPS concentrations <10 ng/mL (Figure 1D). When the treatment duration was changed, 10 ng/mL LPS was found to inhibit L-Glu uptake in a time-dependent manner, and a significant decrease was observed at 72 h (Figure 1E). Therefore, we adopted a 72-h treatment with 10 ng/mL LPS for inflammation without cell death. We also confirmed the morphology and cell density of each cell type in this inflammation model. LPS dramatically changed the shape of Iba-1 (+) microglia from a ramified shape to an amoeboid shape, which is consistent with the typical morphological changes observed after activation of microglia in previous reports [16,17] (Figure 1G). No changes were observed in astrocytes or neurons. The cell densities of all cell types did not change (Figure 1F).

To determine which L-Glu transporter subtypes were responsible for the increase in the concentration of L-Glu remaining in the mixed cultures, we first examined the effects of various subtype-specific inhibitors on L-Glu uptake (Figure 2A). The cultures were treated with a non-selective L-Glu transporter inhibitor (TBOA) (10 to 1,000 μM), a GLAST-specific inhibitor (UCPH-101) (0.1 to 10 μM), or a GLT-1-specific inhibitor (DHK) (30 to 300 μM) for 24 h, and the concentration of L-Glu remaining in the medium 30 min after the application of L-Glu (the starting concentration was 100 μM) in the presence of the inhibitors was measured. TBOA and UCPH-101 increased the L-Glu remaining in a concentration-dependent manner to similar extents, whereas DHK did not. These results indicate that GLAST is the predominant functional transporter in

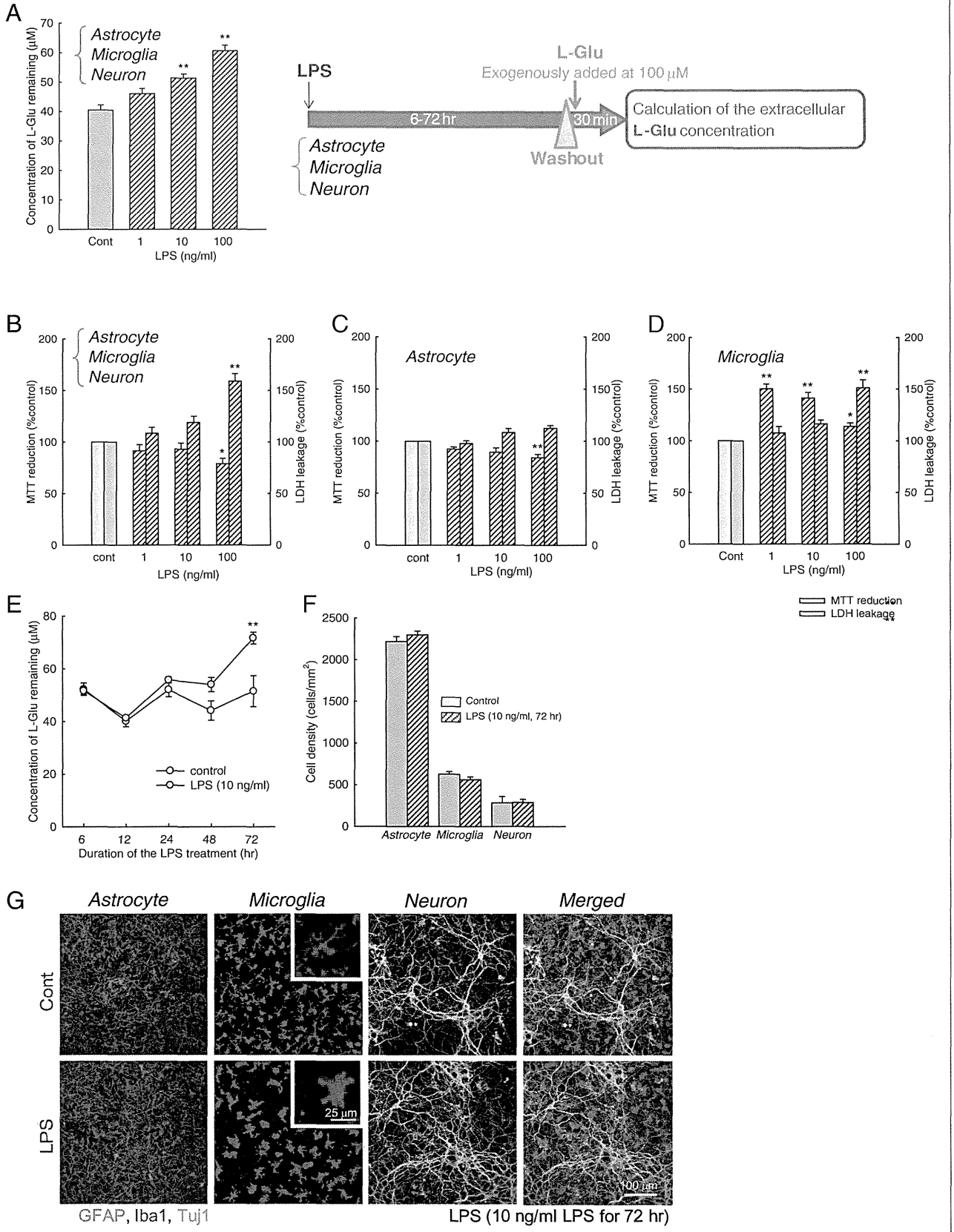

Figure 1 (See legend on next page.)

(See figure on previous page.)

Figure 1 The concentration of L-Glu remaining was increased during inflammation without cell death. (**A**) Effects of LPS (1 to 100 ng/mL, 72 h) on the concentration of L-Glu remaining. The L-Glu remaining was significantly increased after incubation with 10 and 100 ng/mL LPS. $^{**}P < 0.01$ *vs.* control group ($n = 6$), Tukey's test following an ANOVA. (**B**, **C**, **D**) Effects of LPS on LDH leakage and MTT reduction in the astrocyte-microglia-neuron mixed cultures, astrocyte cultures, and microglia cultures. Significant LDH leakage and decreases in MTT reduction were induced by 100 ng/mL LPS but not by LPS concentrations <10 ng/mL in the mixed cultures (B). In the pure astrocyte culture, LPS concentrations <10 ng/mL affected neither LDH leakage nor MTT reduction (C). In the pure microglial culture, significant LDH leakage was induced by 100 ng/mL but not by LPS concentrations <10 ng/mL (**D**). (**E**) Time-dependent effects of LPS. The concentration of L-Glu remaining was measured after 6 to 72-h treatments with LPS (10 ng/mL). $^{**}P < 0.01$ *vs.* control group ($n = 6$), paired *t*-test. (**F**) The effects of LPS (10 ng/mL, 72 h) on the number of neurons, astrocytes, and microglia. LPS treatment had no effect on the cell numbers ($n = 5$). (**G**) Immunostaining of astrocytes, microglia, and neurons in the mixed culture with antibodies against GFAP (red), Iba-1 (blue), and Tuj1 (green) after treatment with 10 ng/mL LPS for 72 h. LPS dramatically changed the shape of the microglia from a ramified shape to an amoeboid shape.

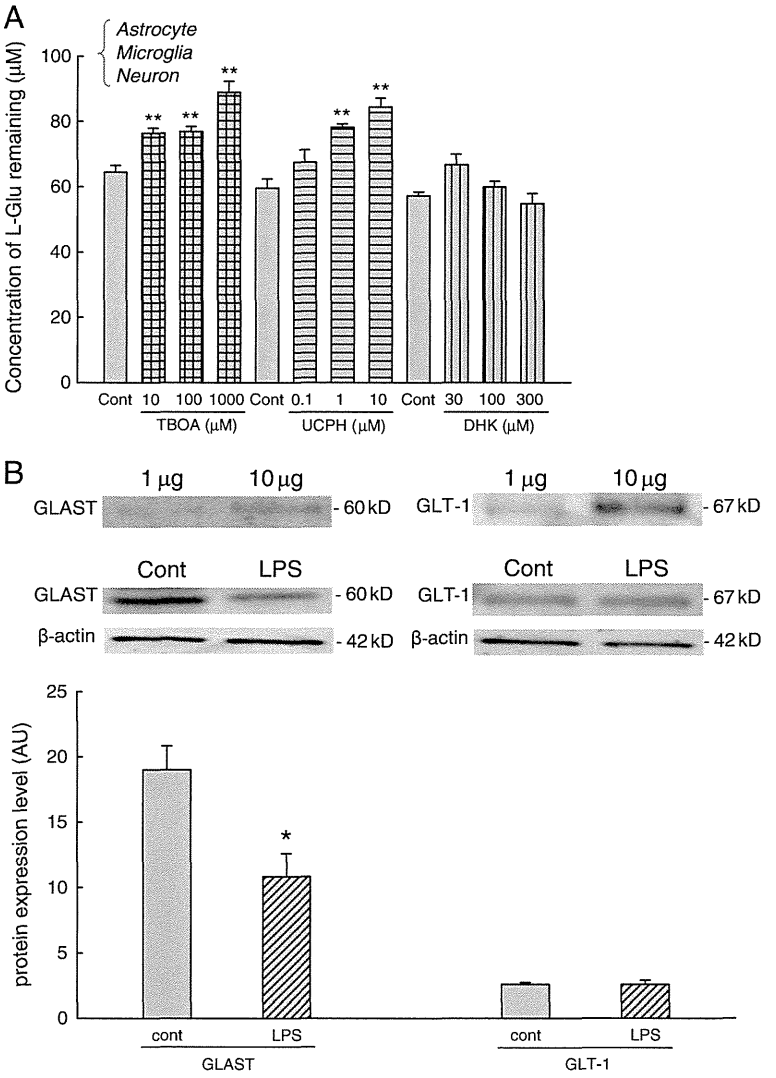

Figure 2 The increase in the concentration of L-Glu remaining was mainly caused by the downregulation of GLAST. (**A**) The effects of TBOA (30 to 300 μM), UCPH-101 (0.1 to 10 μM), and DHK (30 to 300 μM) on L-Glu clearance. Concentration-dependent inhibition was obtained by treatment with TBOA and UCPH-101. $^{**}P < 0.01$ *vs.* the control group ($n = 6$), Tukey's test following ANOVA. (**B**) The basal expression levels of astrocyte L-Glu transporters and the effect of LPS on their expression levels. Basally, the GLAST protein level is much higher than that of GLT1. The GLAST protein levels significantly decreased after the LPS treatment (10 ng/mL, 72 h), but GLT-1 protein levels did not change. $^{*}P < 0.05$ *vs.* the control group ($n = 4$), Student's *t*-test.

the mixed culture. We therefore examined the basal expression levels of astrocyte L-Glu transporters and the effect of LPS on their expression levels. To compare the expression levels of GLAST and GLT1, we first compared the densities of western blotting bands for the same amount of GLAST and GLT1 control proteins (full length) (1, 10 μg) obtained at the same appropriate exposure time (Figure B, upper photos). Then, we quantified the expression levels of GLAST and GLT1 in the control- and LPS-treated mixed culture (Figure B, middle photos). The density of each band obtained at the same appropriate exposure time was normalized to the 10 μg control band of the corresponding subtype. Basally, the GLAST protein level is much higher than that of GLT1 (Figure 2, graph). The GLAST protein levels decreased to 65.7 ± 7.40% of control levels after LPS treatment (10 ng/mL, 72 h) (Figure 2C), but the GLT-1 protein level did not change. These results suggest that the LPS-induced increase in the L-Glu remaining was mainly caused by the downregulation of GLAST.

Activated microglia caused the decrease in L-Glu uptake during inflammation without cell death

To confirm that activated microglia are essential for the decrease in L-Glu uptake during inflammation without cell death, we examined the effects of LPS in four different types of cultures, including an astrocyte-microglia-neuron mixed culture (a), an astrocyte culture (b), an astrocyte-microglia co-culture (c), and an astrocyte-neuron co-culture (d) (Figure 3A). In (a), the astrocytes were confluent, and the cell densities of the microglia and the neurons were 3.0×10^4 cells/cm^2 and 6.0×10^4 cells/cm^2, respectively. Therefore, the cell density of the microglia in (c) and that of neurons in (d) were carefully adjusted to 3.0×10^4 cells/cm^2 and 6.0×10^4 cells/cm^2, respectively. Furthermore, in (b) to (d), we confirmed that the density of each cell type that had been presumably removed was sufficiently low; the number of microglia in (b) and (d) was $<1.2 \times 10^3$ cells/cm^2, and the number of neurons in (b) and (c) was $<1.0 \times 10^3$ cells/cm^2. Astrocytes

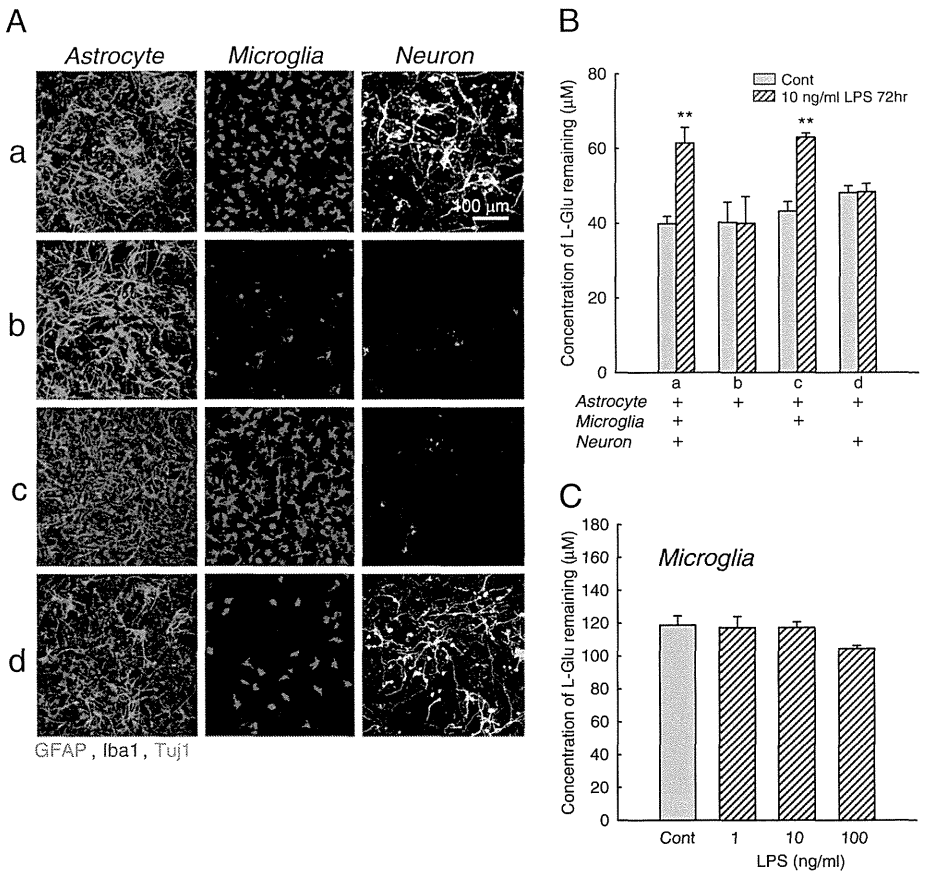

Figure 3 Activated microglia are essential for the decrease in L-Glu uptake in the model of inflammation without cell death. (**A**) Immunostaining of four types of cultures: astrocyte-microglia-neuron mixed culture (a), astrocyte culture (b), astrocyte-microglia co-culture (c), and neuron-astrocyte co-culture (d). (**B**) The effects of LPS (10 ng/mL, 72 h) on the concentration of L-Glu remaining in the four types of culture. Inhibitory effects were obtained in (a) and (c). $^{**}P < 0.01$ *vs.* control group ($n = 6$), Student's *t*-test. (**C**) The effects of LPS (10 ng/mL, 72 h) on the concentration of L-Glu remaining in microglial pure culture. The concentration of L-Glu remaining did not change during the assay (30 min).

were confluent in (a) to (d). When we treated these cultures with LPS (10 ng/mL, 72 h), significant decreases in L-Glu uptake occurred in (a) and (c) but not in (b) nor (d). As shown in Figure 3B (b), the L-Glu uptake in astrocyte pure culture was not changed by LPS. We further confirmed that in the LPS-treated microglial pure culture, the concentration of L-Glu remaining did not change during the assay (30 min) (Figure 3C). These results indicate that the increase in L-Glu remaining, that is, the inhibition of L-Glu uptake, observed in Figure 3B (a) and (c) was caused by the interaction between the activated microglia and the astrocytes during 72 h of LPS treatment.

L-Glu released from activated microglia caused the downregulation of GLAST expression during inflammation without cell death

Activated microglia release various soluble factors in inflammatory processes [16,18-24]. To examine the involvement of these factors in the action of activated microglia on L-Glu transporters, we applied the

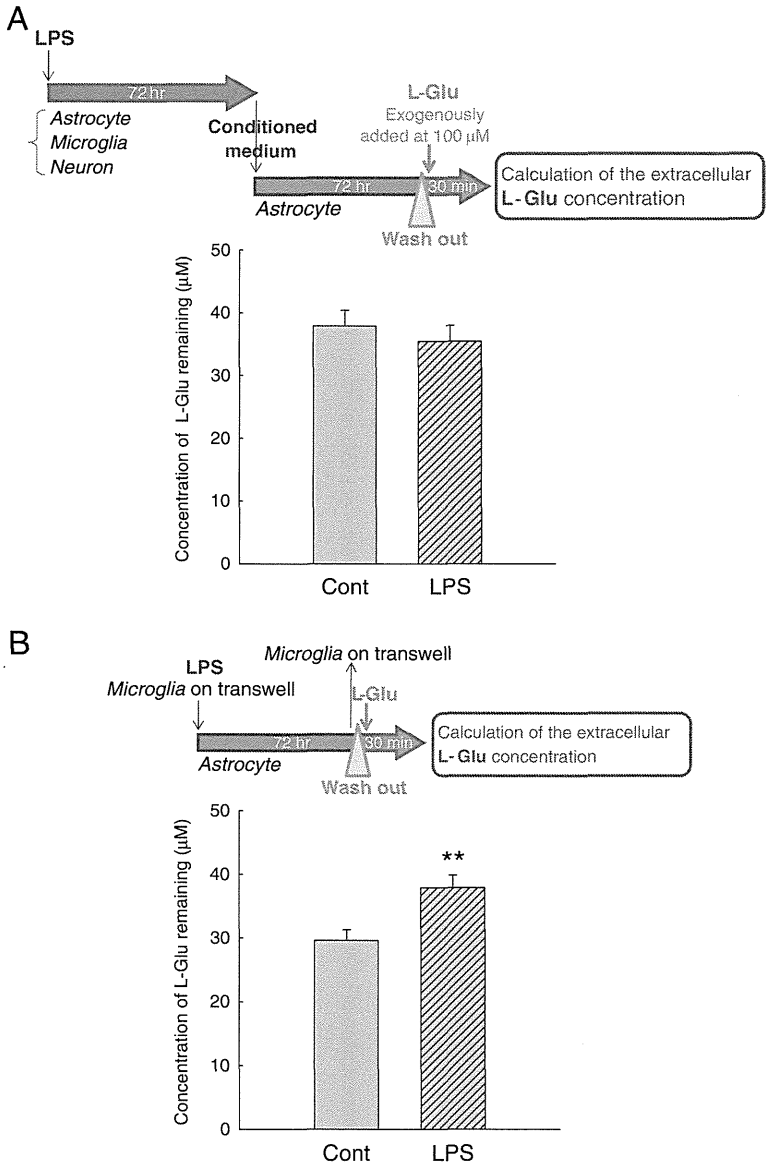

Figure 4 Transwell carrying activated microglia, but not the conditioned medium, decreased L-Glu uptake in the astrocyte culture. (**A**) Effect of the conditioned medium collected from the astrocyte-microglia-neuron mixed culture treated with LPS (10 ng/mL, 72 h) on L-Glu clearance in the astrocyte culture. A 72-h incubation with the conditioned medium did not affect L-Glu clearance in the astrocyte culture. (**B**) The effects of transwell-cultured microglia in the presence of LPS (10 ng/mL, 72 h) on L-Glu uptake in the astrocyte culture. A significant decrease in the L-Glu uptake was caused by 72-h treatment with the transwell. $^{**}P < 0.01$ *vs.* control group ($n = 6$), Student's *t*-test.

conditioned medium collected from the inflammation without cell death model (Figure 4A) to a culture of astrocytes alone. A 72 h-incubation with the conditioned medium did not affect the L-Glu uptake in the astrocyte culture. We then incubated the astrocyte culture with a transwell on which microglia were cultured in the presence of LPS (10 ng/mL, 72 h) (Figure 4B). Notably, a significant decrease in L-Glu uptake was obtained under these conditions. Because LPS in this condition did not directly affect the L-Glu uptake in the astrocyte culture, as shown in Figure 3B (b), these results suggest that the secreted factors are released from microglia and are degraded or taken up after their release. ATP has been shown to downregulate GLAST through the P2X7 receptor [28] and the ectonucleotidases of astrocytes rapidly convert extracellular ATP to ADP, ultimately to AMP [34]. We first examined the contribution of ATP to the downregulation of GLAST in the inflammation model without cell death. Exogenous application of ATP (Figure 5A) and P2X7 agonist BzATP (Figure 5B) did not change the L-Glu uptake. We also confirmed that neither the P2X receptor antagonist TNP-ATP (Figure 5C) nor the P2X7-specific antagonist BBG (Figure 5D) inhibited the decrease in L-Glu uptake in this inflammation model. We then examined the possibility of L-Glu. L-Glu is released by activated microglia through hemichannels [21,22] and taken up by L-Glu transporters after its release. We hypothesized that the secreted factor may be L-Glu. We first examined whether L-Glu was indeed released from microglia during inflammation without cell death. As shown in Figure 6A, left, LPS elevated the extracellular L-Glu concentrations in the astrocyte-microglia-neuron mixed cultures, and a significant elevation was observed even at a concentration of 1 ng/mL (Figure 6A left). An elevation of the extracellular L-Glu concentration was observed in

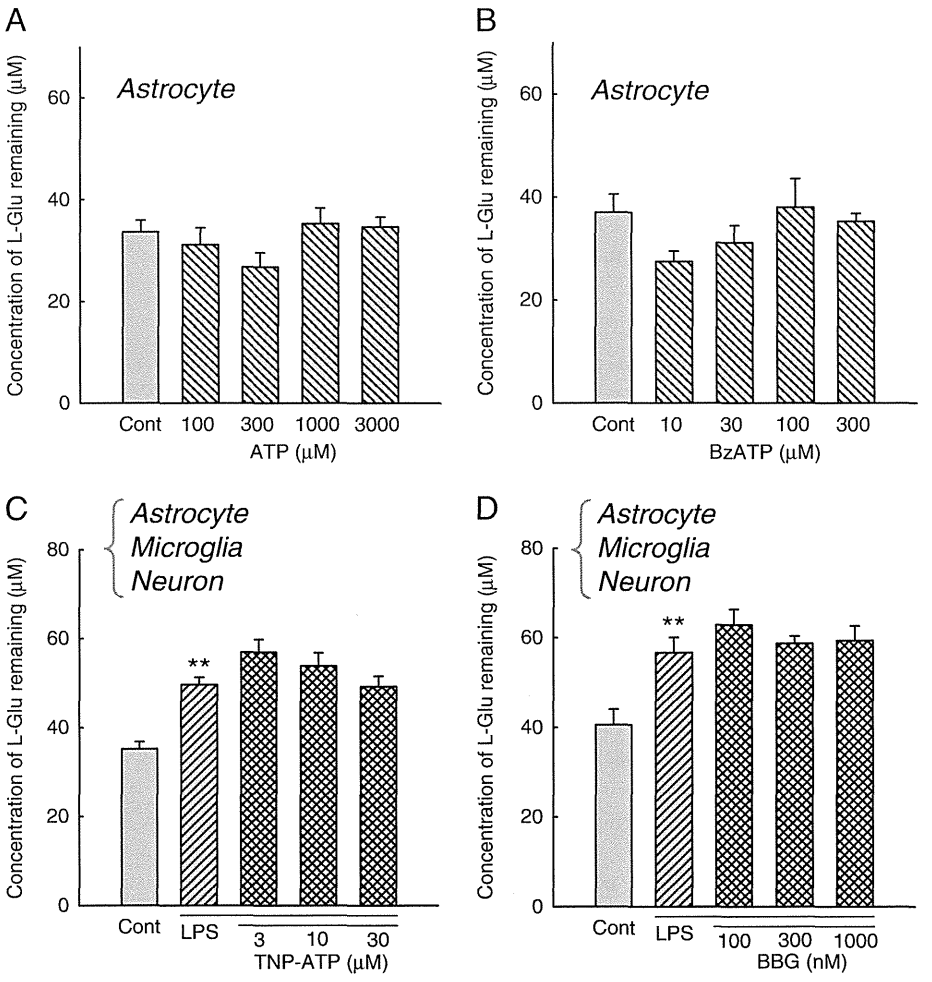

Figure 5 ATP did not contribute to the downregulation of GLAST in the inflammation without cell death. (**A**, **B**) Neither ATP nor the P2X7 agonist BzATP affected L-Glu uptake. (**C**, **D**) Neither the P2X receptor antagonist TNP-ATP nor the P2X7 specific antagonist BBG affected the LPS-induced decrease in L-Glu uptake. $^{**}P < 0.01$ *vs.* control group ($n = 6$), Tukey's test following ANOVA.

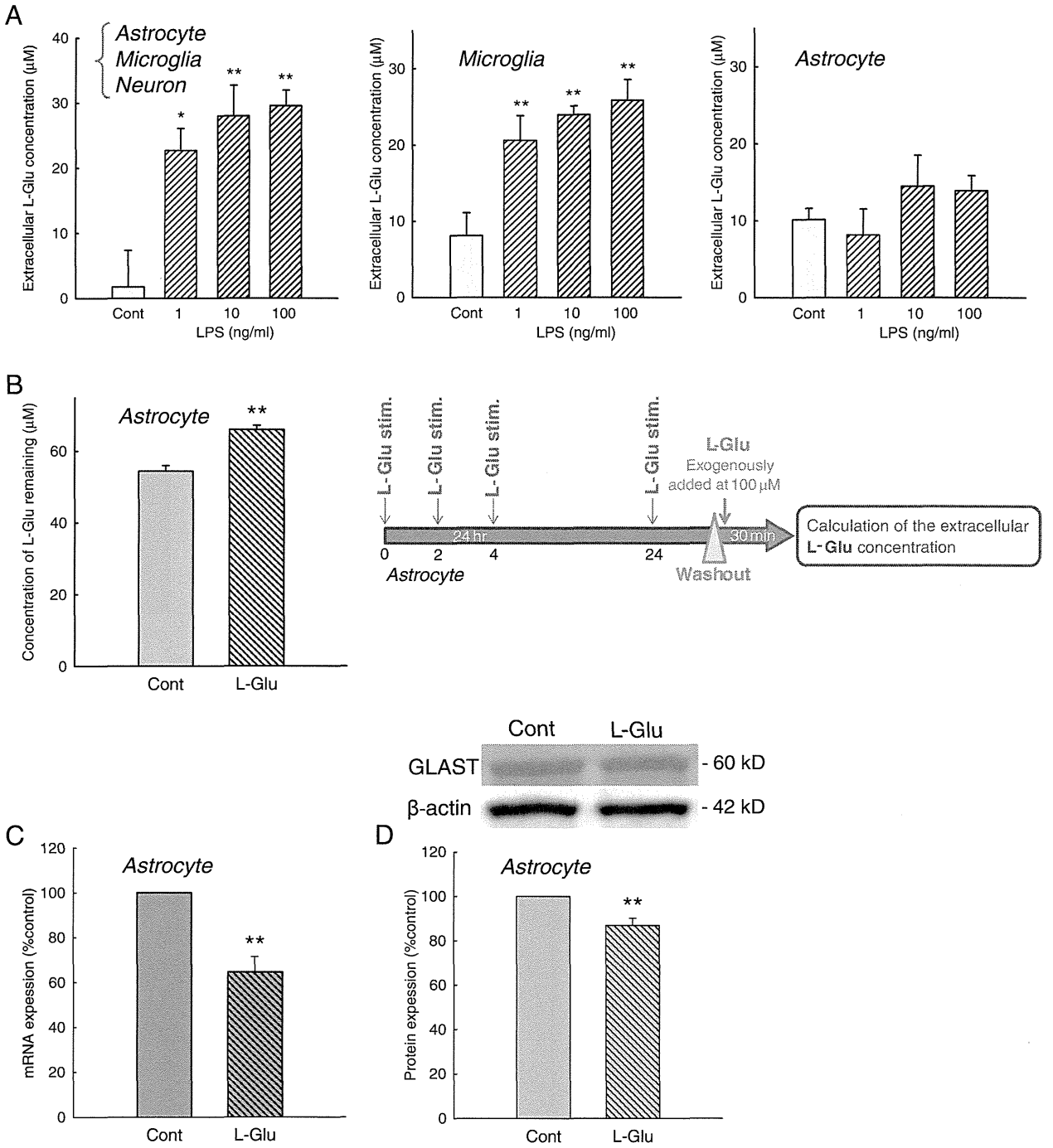

Figure 6 L-Glu released from activated microglia caused the downregulation of GLAST. (**A**) Effects of LPS (1 to 100 ng/mL, 24 h) on the extracellular concentration of L-Glu in the astrocyte-microglia-neuron mixed culture (left), microglia culture (center), and astrocyte culture (right). LPS significantly increased the extracellular L-Glu in the astrocyte-microglia-neuron mixed culture and the microglia culture. $^{*}P < 0.05$, $^{**}P < 0.01$ *vs.* control group ($n = 6$), Tukey's test following ANOVA. (**B**) The effect of sustained exposure to L-Glu on L-Glu clearance in the astrocyte culture. The culture medium was changed to fresh medium containing 100 μM L-Glu every 2 h. L-Glu clearance was suppressed by sustained exposure to L-Glu for 24 h. $^{**}P < 0.01$ *vs.* the control group ($n = 6$), Student's *t*-test. (**C**) The effect of sustained exposure to L-Glu on GLAST mRNA levels. Sustained exposure to L-Glu decreased GLAST mRNA. $^{**}P < 0.01$ *vs.* control group ($n = 4$), Student's *t*-test. (**D**) The effect of sustained exposure to L-Glu on GLAST protein levels. Sustained exposure to L-Glu decreased the protein expression of GLAST. $^{**}P < 0.01$ *vs.* control group ($n = 5$), Student's *t*-test.

the microglia culture (Figure 6A center) but not in the astrocyte culture (Figure 6A right). These results indicate that L-Glu was released from activated microglia during inflammation without cell death. To confirm our hypothesis, we tested the effect of the sustained elevation of extracellular L-Glu on L-Glu uptake in the mixed culture. To yield a sustained elevation of extracellular L-Glu, the culture medium of the astrocyte culture was freshly supplemented with 100 μM L-Glu every 2 h for 24 h, as preliminary studies showed that a concentration of 100 μM extracellular L-Glu was reduced to almost zero after 4 h in confluent astrocyte cultures (not shown). As shown in Figure 6B, the sustained elevation of extracellular L-Glu resulted in a significant decrease in L-Glu uptake in the astrocyte culture. GLAST expression was significantly decreased at the mRNA level

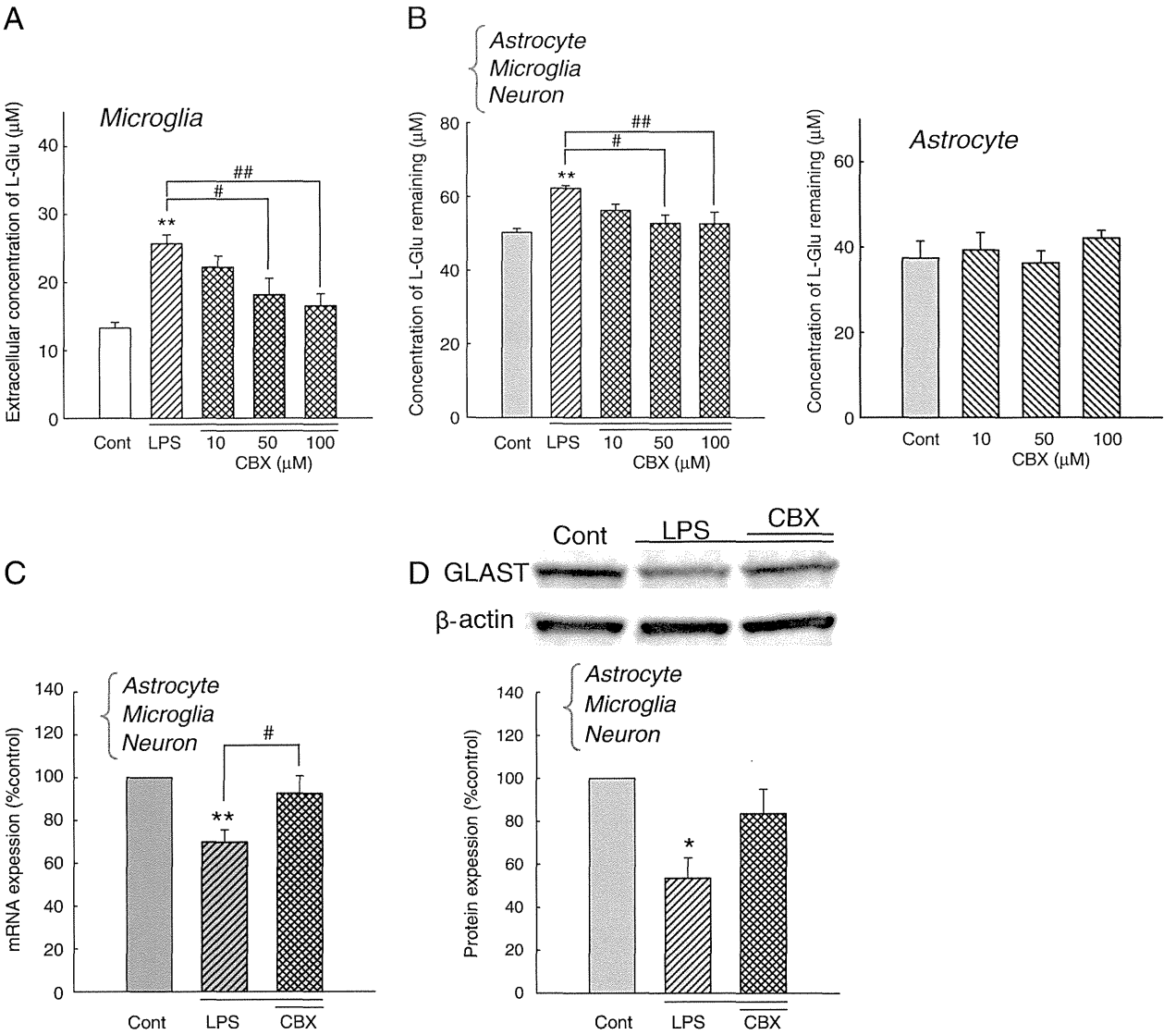

Figure 7 CBX ameliorated the decrease in L-Glu uptake and GLAST expression in inflammation without cell death. (**A**) The effect of CBX on L-Glu release from activated microglia. CBX concentration-dependently suppressed L-Glu release due to LPS (10 ng/mL, 24 h)-activated microglia. $^{**}P < 0.01$ *vs.* control group, $\#P < 0.05$, $\#\#P < 0.01$ *vs.* the LPS-treated group ($n = 5$), Tukey's test following ANOVA. (**B**) The effects of CBX on the decreased L-Glu uptake in the model of inflammation without cell death. CBX concentration-dependently inhibited the LPS (10 ng/mL, 72 h)-induced decrease in L-Glu uptake in the astrocyte-microglia-neuron mixed culture (left) but not in the astrocyte culture (right). $^{**}P < 0.01$ *vs.* control group, $\#P < 0.05$, $\#\#P < 0.01$ *vs.* the LPS-treated group ($n = 5$), Tukey's test following ANOVA. (**C**) The effect of CBX on the LPS-induced decrease in GLAST mRNA levels. In the presence of CBX (100 μM), the LPS (10 ng/mL, 24 h)-induced decrease in GLAST mRNA level was ameliorated in the astrocyte-microglia-neuron mixed culture. $^{**}P < 0.01$ *vs.* control group, $\#P < 0.05$ *vs.* the LPS-treated group ($n = 5$), Tukey's test following ANOVA. (**D**) The effect of CBX on the LPS-induced decrease in GLAST protein levels. In the presence of CBX (100 μM), the LPS (10 ng/mL, 72 h)-induced decrease in GLAST protein levels was ameliorated in the astrocyte-microglia-neuron mixed culture. $^{*}P < 0.05$ *vs.* control group ($n = 4$), Tukey's test following ANOVA.

(Figure 6C) and the protein level (Figure 6D) by the same treatment. These results suggest that L-Glu was responsible for the decrease in L-Glu uptake during inflammation without cell death. When the microglia cultures were treated with LPS (10 ng/mL, 24 h) in the absence or presence of the hemichannel inhibitor, CBX (10 to 100 μM), the L-Glu release from the activated microglia was suppressed in a concentration-dependent manner (Figure 7A). CBX (100 μM) almost completely prevented the LPS-induced (10 ng/mL, 72 h) decrease in L-Glu uptake in the mixed culture (Figure 7B, left) but had no effect in the astrocyte culture (Figure 7B, right). Furthermore, CBX reversed the LPS-induced downregulation of GLAST expression at the mRNA (Figure 7C) and protein levels (Figure 7D).

We next tried to clarify the mechanisms through which the sustained elevation of extracellular L-Glu downregulates GLAST. Recent reports have suggested that the expression of L-Glu transporters is regulated by L-Glu through metabotropic glutamate receptors (mGluRs). We therefore first examined the involvement of metabotropic glutamate receptors (mGluRs). Neither the group I mGluR agonist DHPG nor the group II mGluR agonist DCG-4 affected either L-Glu uptake

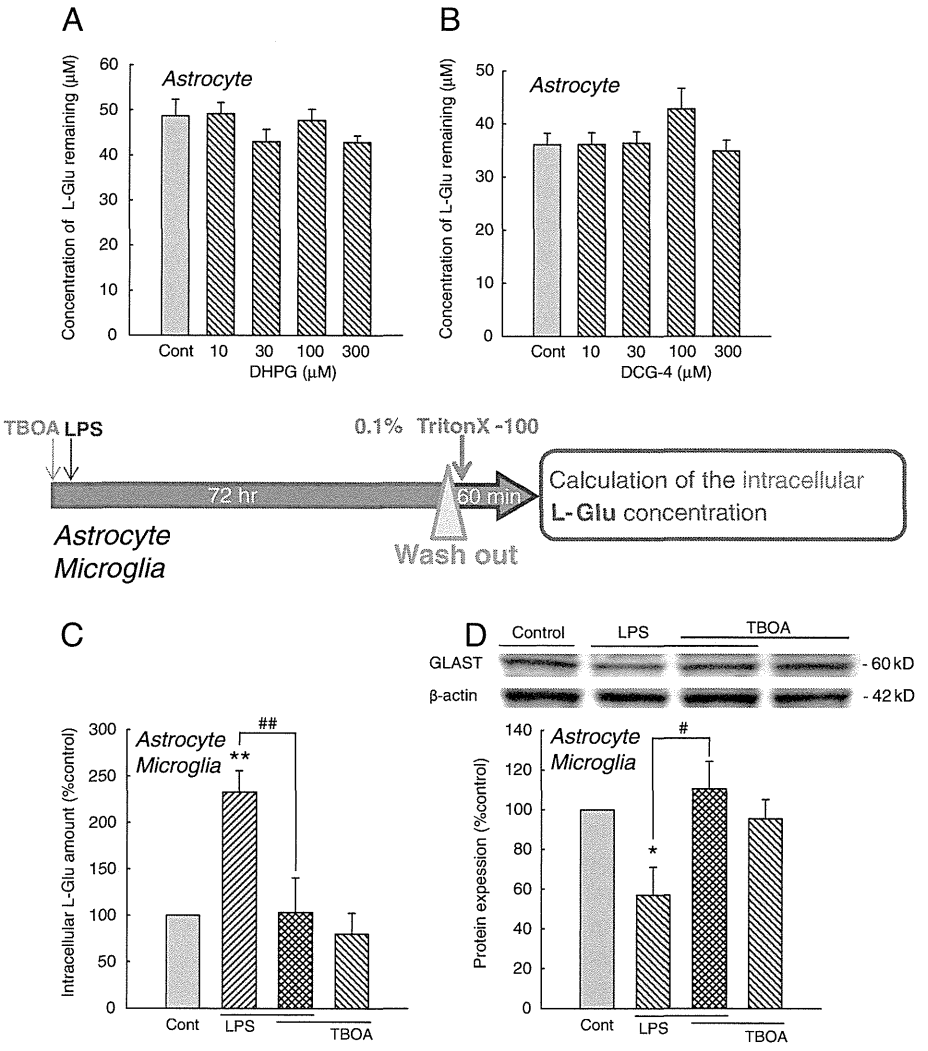

Figure 8 The elevation of intracellular L-Glu in astrocytes is important for the downregulation of GLAST. (**A**, **B**) The effects of mGluR agonists on L-Glu uptake. Neither the group I mGluR agonist DHPG (A) nor the group II mGluR agonist DCG-4 (B) affected L-Glu uptake. (**C**) The amount of astrocytic intracellular L-Glu after LPS-treatment in the absence or presence of TBOA in astrocyte-microglia co-cultures. LPS significantly increased the amount of astrocytic intracellular L-Glu, and TBOA completely suppressed this increase. $^{**}P < 0.01$ *vs.* control group, $\#\#P < 0.01$ *vs.* the LPS-treated group ($n = 6$), Tukey's test following ANOVA. (**D**) The astrocytic expression of GLAST after LPS treatment in the absence or presence of TBOA in astrocyte-microglia co-cultures. TBOA suppressed the downregulation GLAST caused by LPS. $^{*}P < 0.05$ *vs.* control group, $\#P < 0.05$ *vs.* the LPS-treated group ($n = 6$), Tukey's test following ANOVA.

(Figure 8A and B) or the expression level of GLAST (not shown). Sustained elevation of extracellular L-Glu caused by activated microglia is expected to cause the elevation of intracellular L-Glu in astrocytes. We therefore examined whether the elevation of intracellular L-Glu itself is important for the downregulation of GLAST. To do this, we first measured the amount of astrocytic intracellular L-Glu after LPS-treatment in the absence or presence of TBOA in astrocyte-microglia co-cultures (Figure 8C). LPS significantly increased the amount of intracellular L-Glu, and TBOA completely suppressed this increase. Western blotting showed that TBOA suppressed the downregulation GLAST caused by LPS (Figure 8D). TBOA itself did not have effects on either the amount of intracellular L-Glu or the GLAST protein level. These results indicate that the elevation of astrocytic intracellular L-Glu, but not the signaling cascade from the cell surface, is important for the downregulation of GLAST.

Our findings suggest that activated microglia trigger the elevation of extracellular L-Glu through their own release of L-Glu, astrocyte L-Glu transporters are downregulated by the elevation of astrocytic intracellular L-Glu, and further elevation of extracellular L-Glu occurs early in neuroinflammation. A schematic model of this 'collusion' hypothesis is shown in Figure 9.

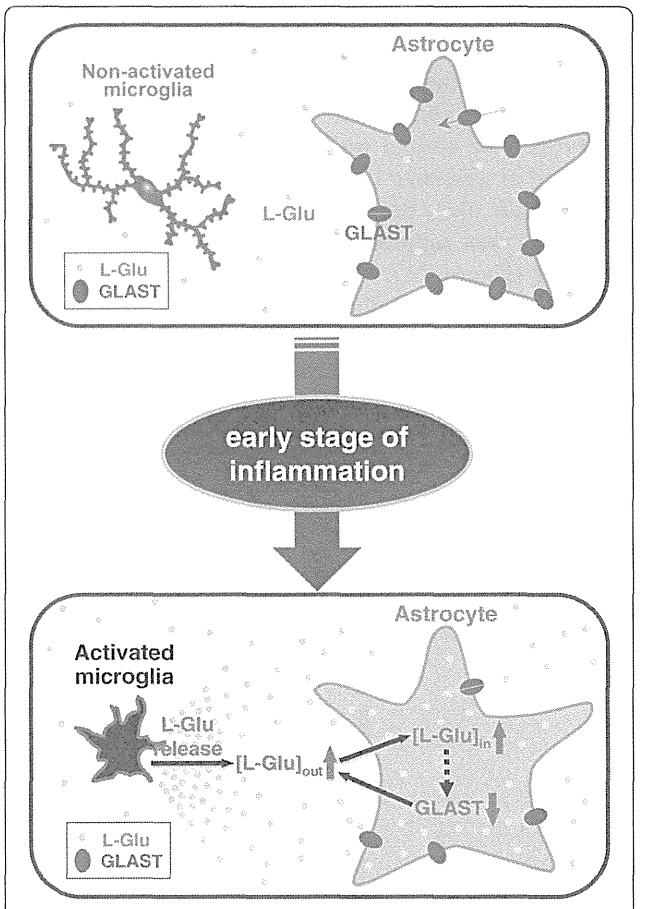

Figure 9 Schematic model of the 'collusion' hypothesis for the elevation of extracellular L-Glu in the early stages of inflammation. 1. Activated microglia release L-Glu. 2. The resultant elevation of extracellular L-Glu causes the elevation of astrocytic intracellular L-Glu. 3. The elevation of astrocytic intracellular L-Glu downregulates GLAST expression. 4. The decrease in GLAST expression further exacerbates the elevation of extracellular L-Glu.

Discussion

To quantify L-Glu transporter function, we measured the extracellular concentrations of L-Glu 30 min after a single exogenous application of L-Glu to the medium (the starting concentration was 100 μM). To limit any contributions of extra L-Glu from dying cells, and to verify a substantial contribution of the decrease in L-Glu transport potency to an elevated concentration of extracellular L-Glu in inflammation, we first determined the optimal conditions for inflammation without cell death. We used a lower concentration of LPS (10 ng/mL) than is generally used [35,36]. LPS application at a concentration of 10 ng/mL for 72 h activated the microglia but did not cause either LDH leakage or decreases in MTT reduction in the mixed culture, astrocyte pure culture, or microglia pure culture. LPS induces an inflammatory response in microglia via Toll-like receptor 4 (TLR4) [37]. TLR4 is also expressed by astrocytes, and astrocytes themselves have shown inflammatory responses in response to LPS in some reports [38]. In the present study, however, microglia were essential for the decreased L-Glu by astrocytes, and LPS did not affect L-Glu uptake in astrocyte cultures. Because the expression of TLR4 by astrocytes is less than that of microglia [37], the LPS stimulation in our model of inflammation without cell death may be insufficient to induce phenotypic changes in astrocytes. These mild inflammatory conditions may reflect the early stages of neuroinflammation *in vivo*, in which early microglial activation has been observed to precede the phenotypic changes in astrocytes [39].

In the present study, we pharmacologically confirmed that GLAST, and not GLT-1, was the predominant functional L-Glu transporter. We also confirmed that the expression level of GLT-1 is much lower than that of GLAST. GLT-1 has been reported to be functional in neuron-astrocyte co-cultures at 32 to 44 DIV [40]. This discrepancy most likely arises from the maturation stages of neurons, as the functional development of GLT-1 correlates with neuronal maturation [41]. The expression of GLAST was significantly decreased in the 'non-cell death inflammation model', which indicates that the decrease in L-Glu uptake in this inflammation model was mainly caused by the downregulation of GLAST.

Activated microglia release various soluble factors, including inflammatory cytokines [18,19], reactive oxygen species [20], NO [16], L-Glu [21,22], and ATP [23,24]. We demonstrated that L-Glu is the factor that downregulates GLAST in astrocytes during inflammation without cell death. Although activated microglia are known to release L-Glu through hemichannels [21,22], the neurological importance of this phenomenon remains unclear. We showed that the hemichannel inhibitor CBX completely suppressed the release of L-Glu from microglia, the decrease in L-Glu uptake, and the downregulation of GLAST expression during inflammation without cell death. These data provide strong evidence that L-Glu is the microglial releasing factor that downregulates GLAST. High concentrations of ATP have also been shown to downregulate GLAST through the P2X7 receptor [28]. However, we believe that ATP did not contribute to the down-regulation of GLAST in the inflammation model without cell death here because L-Glu uptake did not change when the astrocyte culture was treated with ATP (Figure 5A) or the P2X7 agonist BzATP (Figure 5B). We also confirmed that neither the P2X receptor antagonist TNP-ATP (Figure 5C) nor the P2X7-specific antagonist BBG (Figure 5D) inhibited the decrease in L-Glu uptake in this inflammation model. Other microglial releasing factors, such as TNF-α, IL-1β, and arachidonic acid, are also known to decrease the L-Glu transport in astrocyte cultures [25-27]. However, the conditioned media collected from our model of inflammation without cell death had no effect in the astrocyte culture. Because the LPS stimulation here was lower than that of other studies [35,36] (to prevent cell death), the amount of these factors in the conditioned media may have been insufficient to affect L-Glu transporters.

Recent reports have suggested that the expression of L-Glu transporters is regulated by L-Glu through metabotropic glutamate receptors (mGluRs), that is, the group I mGluR agonist downregulates GLAST, whereas the group II mGluR agonist has the opposite effect [42,43]. However, neither the group I mGluR agonist nor the group II mGluR agonist affected the expression of GLAST in the present study. Instead, we clarified that the elevation of intracellular L-Glu in astrocytes is important for the downregulation of GLAST as shown in Figure 8. It has been clarified that translation initiation is regulated by intracellular L-Glu transported by GLAST in Bergmann glial cells [44,45]. They also showed that mammalian target of rapamycin (mTOR), increase in intracellular Ca^{2+} levels, and p60(Src)/PI3K/PKB pathway are involved in this regulation. Further investigation is necessary to confirm whether the same pathways are involved in the downregulation of GLAST observed in our study. Of interest, a sustained elevation of extracellular L-Glu induced by the same protocol as Figure 6 did not cause the downregulation of glutamine synthetase (GS) in our preliminary experiment (data not shown), suggesting that this regulation is GLAST or L-Glu transporter-specific. The comparison of the upstream DNA sequences of GLAST and GS might provide useful information. Besides, in *Saccharomyces cerevisiae*, the activator (NIL1p) of the amino acid transporter is inactivated by increases in intracellular glutamate [46]. It is possible that a conserved mechanism similar to this also exist in astrocytes. Our findings strongly suggest that L-Glu is the microglial releasing factor which results in downregulation of GLAST in the early stage of inflammation. However, whether or not the quantity of L-Glu released from microglia is enough to induce a range of reaction still needs to be elucidated. Based on the discussion above, the co-factors to enhance the signaling pathway in the astrocytes leading to the downregulation of GLAST might be also released from microglia.

Conclusions

Our findings suggest that activated microglia trigger the elevation of extracellular L-Glu through their own release of L-Glu, astrocyte L-Glu transporters are downregulated by the elevation of astrocytic intracellular L-Glu, and further elevation of extracellular L-Glu is caused as an early event of neuroinflammation (Figure 9).

Abbreviations

ANOVA: Analysis of variance; ATP: Adenosine 5′-triphosphate disodium salt hydrate; BPB: Bromophenol blue sodium salt; BSA: Albumin bovine serum; BzATP: 2′ (3′)-O-(4-Benzoylbenzoyl)ATP triethylammonium salt; CBX: Carbenoxolone; CNS: Central nervous system; DHK: Dihydrokainic acid; DIV: Days *in vitro*; DMEM: Dulbecco's modified eagle medium; DNA: Deoxyribonucleic acid; EDTA: Ethylenediaminetetraacetate; EGTA: Ethyleneglycoldiaminetetraacetate; FBS: Fetal bovine serum; GFAP: Glial fibrillary acidic protein; GIDH: Glutamate dehydrogenase; HS: Horse serum; LDH: Lactate dehydrogenase; L-Glu: L-glutamate; LPS: Lipopolysaccharide; mGluRs: Metabotropic glutamate receptors; MPMS: 1-methoxy-5-methylphenazinium methyl sulfate; MTT: 3-(4,5-dimethyl-2-thiazolyl)-2,5-diphenyl-2H-tetrazolium bromide; β-NAD: β-nicotinamide adenine dinucleotide; NO: Nitric oxide; NP-40: Polyoxyethylene(9)octylphenyl ether; OxATP: Adenosine 5′-triphosphate periodate oxidized sodium salt; PBS: Phosphate-buffered saline; PFA: Paraformaldehyde; RNA: Ribonucleic acid; RT-PCR: Polymerase chain reaction; SD: Sprague–Dawley; SDS: Sodium dodecyl sulfate; TBOA: DL-threo-β-benzyloxyaspartic acid; TLR4: Toll-like receptor 4; TNP-ATP: 2′,3′-O-(2,4,6-Trinitrophenyl)ATP salt hydrate; Tris–HCl: Tris (hydroxymethyl) aminomethane; Tuj1: β3 tubulin; UCPH 101: 2-Amino-5,6,7,8-tetrahydro-4-(4-methoxyphenyl)-7-(naphthalen-1-yl)-5-oxo-4H-chromene-3-carbonitrile.

Competing interests

I declare that I have no significant competing financial, professional or personal interests that might have influenced the performance or presentation of the work described in this manuscript.

Authors' contributions

JT performed experimental work and manuscript writing. KF performed experimental work. MM performed additional experimental work. TS provided advice on the experimental direction. YS provided advice on manuscript writing and preparation. KS designed the biological experimental plan and performed biological experiments, data analysis, manuscript writing, and preparation. All authors have read and approved the final version of the manuscript.

Acknowledgements

This study was partly supported by a Grant-in-Aid from the Food Safety Commission of Japan (No. 1003); a Grant-in-Aid for Young Scientists from MEXT, Japan (KAKENHI 21700422); the Program for the Promotion of Fundamental Studies in Health Sciences of NIBIO, Japan; a Health and Labor Science Research Grant for Research on Risks of Chemicals; and a Health and Labor Science Research Grant for Research on New Drug Development from MHLW, Japan, awarded to KS and YS.

Author details

[1]Laboratory of Neuropharmacology, Division of Pharmacology, National Institute of Health Sciences, 1-18-1 Kamiyoga, Setagaya-ku, Tokyo 158-8501, Japan. [2]Division of Basic Biological Science, Faculty of Pharmacy, Keio University, 1-5-30 Shiba-koen, Minato-ku, Tokyo 105-8512, Japan.

Received: 25 May 2012 Accepted: 1 December 2012
Published: 23 December 2012

References

1. Kumar A, Singh RL, Babu GN: **Cell death mechanisms in the early stages of acute glutamate neurotoxicity.** *Neurosci Res* 2010, **66**:271–278.
2. Choi DW: **Glutamate neurotoxicity and diseases of the nervous system.** *Neuron* 1988, **1**:623–634.
3. Rothstein JD, Dykes-Hoberg M, Pardo CA, Bristol LA, Jin L, Kuncl RW, Kanai Y, Hediger MA, Wang Y, Schielke JP, Welty DF: **Knockout of glutamate transporters reveals a major role for astroglial transport in excitotoxicity and clearance of glutamate.** *Neuron* 1996, **16**:675–686.
4. Lauderback CM, Harris-White ME, Wang Y, Pedigo NW Jr, Carney JM, Butterfield DA: **Amyloid beta-peptide inhibits Na^+-dependent glutamate uptake.** *Life Sci* 1999, **65**:1977–1981.
5. Rothstein JD: **Excitotoxicity and neurodegeneration in amyotrophic lateral sclerosis.** *Clin Neurosci* 1995–1996, **3**:348–359.
6. Choudary PV, Molnar M, Evans SJ, Tomita H, Li JZ, Vawter MP, Myers RM, Bunney WE Jr, Akil H, Watson SJ, Jones EG: **Altered cortical glutamatergic and GABAergic signal transmission with glial involvement in depression.** *Proc Natl Acad Sci USA* 2005, **102**:15653–15658.
7. Beart PM, O'Shea RD: **Transporters for L-glutamate: an update on their molecular pharmacology and pathological involvement.** *Br J Pharmacol* 2007, **150**:5–17.
8. Guo F, Sun F, Yu JL, Wang QH, Tu DY, Mao XY, Liu R, Wu KC, Xie N, Hao LY, Cai JQ: **Abnormal expressions of glutamate transporters and metabotropic glutamate receptor 1 in the spontaneously epileptic rat hippocampus.** *Brain Res Bull* 2010, **81**:510–516.
9. Rakhade SN, Loeb JA: **Focal reduction of neuronal glutamate transporters in human neocortical epilepsy.** *Epilepsia* 2008, **49**:226–236.
10. Proper EA, Hoogland G, Kappen SM, Jansen GH, Rensen MG, Schrama LH, van Veelen CW, van Rijen PC, van Nieuwenhuizen O, Gispen WH, de Graan PND: **Distribution of glutamate transporters in the hippocampus of patients with pharmaco-resistant temporal lobe epilepsy.** *Brain* 2002, **125**:32–43.
11. Ward RJ, Colivicchi MA, Allen R, Schol F, Lallemand F, de Witte P, Ballini C, Corte LD, Dexter D: **Neuro-inflammation induced in the hippocampus of 'binge drinking' rats may be mediated by elevated extracellular glutamate content.** *J Neurochem* 2009, **111**:1119–1128.
12. Castillo J, Dávalos A, Alvarez-Sabín J, Pumar JM, Leira R, Silva Y, Montaner J, Kase CS: **Molecular signatures of brain injury after intracerebral hemorrhage.** *Neurology* 2002, **58**:624–629.
13. Allen NJ, Barres BA: **Neuroscience: Glia - more than just brain glue.** *Nature* 2009, **457**:675–677.
14. Lehnardt S: **Innate immunity and neuroinflammation in the CNS: the role of microglia in Toll-like receptor-mediated neuronal injury.** *Glia* 2010, **58**:253–263.
15. Perry VH, Nicoll JA, Holmes C: **Microglia in neurodegenerative disease.** *Nat Rev Neurol* 2010, **6**:193–201.
16. Kreutzberg GW: **Microglia: a sensor for pathological events in the CNS.** *Trends Neurosci* 1996, **19**:312–318.
17. Lynch MA: **The multifaceted profile of activated microglia.** *Mol Neurobiol* 2009, **40**:139–156.
18. Hanisch UK: **Microglia as a source and target of cytokines.** *Glia* 2002, **40**:140–155.
19. Nakajima K, Kohsaka S: **Microglia: activation and their significance in the central nervous system.** *J Biochem* 2001, **130**:169–175.
20. Block ML, Hong JS: **Chronic microglial activation and progressive dopaminergic neurotoxicity.** *Biochem Soc Trans* 2007, **35**:1127–1132.
21. Takeuchi H, Jin S, Wang J, Zhang G, Kawanokuchi J, Kuno R, Sonobe Y, Mizuno T, Suzumura A: **Tumor necrosis factor-alpha induces neurotoxicity via glutamate release from hemichannels of activated microglia in an autocrine manner.** *J Biol Chem* 2006, **281**:21362–21368.
22. Yawata I, Takeuchi H, Doi Y, Liang J, Mizuno T, Suzumura A: **Macrophage-induced neurotoxicity is mediated by glutamate and attenuated by glutaminase inhibitors and gap junction inhibitors.** *Life Sci* 2008, **82**:1111–1116.
23. Higashi Y, Segawa S, Matsuo T, Nakamura S, Kikkawa Y, Nishida K, Nagasawa K: **Microglial zinc uptake via zinc transporters induces ATP release and the activation of microglia.** *Glia* 2011, **59**:1933–1945.
24. Kim SY, Moon JH, Lee HG, Kim SU, Lee YB: **ATP released from beta-amyloid-stimulated microglia induces reactive oxygen species production in an autocrine fashion.** *Exp Mol Med* 2007, **39**:820–827.
25. Carmen J, Rothstein JD, Kerr DA: **Tumor necrosis factor-alpha modulates glutamate transport in the CNS and is a critical determinant of outcome from viral encephalomyelitis.** *Brain Res* 2009, **1263**:143–154.
26. Prow NA, Irani DN: **The inflammatory cytokine, interleukin-1 beta, mediates loss of astroglial glutamate transport and drives excitotoxic motor neuron injury in the spinal cord during acute viral encephalomyelitis.** *J Neurochem* 2008, **105**:1276–1286.
27. Volterra A, Trotti D, Racagni G: **Glutamate uptake is inhibited by arachidonic acid and oxygen radicals via two distinct and additive mechanisms.** *Mol Pharmacol* 1994, **46**:986–992.
28. Liu YP, Yang CS, Chen MC, Sun SH, Tzeng SF: **Ca(2+)-dependent reduction of glutamate aspartate transporter GLAST expression in astrocytes by P2X(7) receptor-mediated phosphoinositide 3-kinase signaling.** *J Neurochem* 2010, **113**:213–227.
29. Sato K, Matsuki N, Ohno Y, Nakazawa K: **Estrogens inhibit l-glutamate uptake activity of astrocytes via membrane estrogen receptor alpha.** *J Neurochem* 2003, **86**:1498–1505.
30. Sato K, Saito Y, Oka J, Ohwada T, Nakazawa K: **Effects of tamoxifen on L-glutamate transporters of astrocytes.** *J Pharmacol Sci* 2008, **107**:226–230.
31. Nakajima K, Shimojo M, Hamanoue M, Ishiura S, Sugita H, Kohsaka S: **Identification of elastase as a secretory protease from cultured rat microglia.** *J Neurochem* 1992, **58**:1401–1408.
32. Kohl A, Dehghani F, Korf HW, Hailer NP: **The bisphosphonate clodronate depletes microglial cells in excitotoxically injured organotypic hippocampal slice cultures.** *Exp Neurol* 2003, **181**:1–11.
33. Abe K, Matsuki N: **Measurement of cellular 3-(4,5-dimethylthiazol-2-yl)-2,5-diphenyltetrazolium bromide (MTT) reduction activity and lactate dehydrogenase release using MTT.** *Neurosci Res* 2000, **38**:325–329.
34. Wink MR, Braganhol E, Tamajusuku AS, Lenz G, Zerbini LF, Libermann TA, Sévigny J, Battastini AM, Robson SC: **Nucleoside triphosphate diphosphohydrolase-2 (NTPDase2/CD39L1) is the dominant ectonucleotidase expressed by rat astrocytes.** *Neuroscience* 2006, **138**:421–432.
35. Li J, Ramenaden ER, Peng J, Koito H, Volpe JJ, Rosenberg PA: **Tumor necrosis factor alpha mediates lipopolysaccharide-induced microglial toxicity to developing oligodendrocytes when astrocytes are present.** *J Neurosci* 2008, **28**:5321–5330.
36. Bal-Price A, Brown GC: **Inflammatory neurodegeneration mediated by nitric oxide from activated glia-inhibiting neuronal respiration, causing glutamate release and excitotoxicity.** *J Neurosci* 2001, **21**:6480–6491.
37. Lehnardt S, Lachance C, Patrizi S, Lefebvre S, Follett PL, Jensen FE, Rosenberg PA, Volpe JJ, Vartanian T: **The toll-like receptor TLR4 is necessary for lipopolysaccharide-induced oligodendrocyte injury in the CNS.** *J Neurosci* 2002, **22**:2478–2486.
38. Carpentier PA, Begolka WS, Olson JK, Elhofy A, Karpus WJ, Miller SD: **Differential activation of astrocytes by innate and adaptive immune stimuli.** *Glia* 2005, **49**:360–374.
39. Tilleux S, Hermans E: **Neuroinflammation and regulation of glial glutamate uptake in neurological disorders.** *J Neurosci Res* 2007, **85**:2059–2070.
40. Swanson RA, Liu J, Miller JW, Rothstein JD, Farrell K, Stein BA: **Longuemare MC: Neuronal regulation of glutamate transporter subtype expression in astrocytes.** *J Neurosci* 1997, **17**:932–940.

41. Perego C, Vanoni C, Bossi M, Massari S, Basudev H, Longhi R, Pietrini G: **The GLT1 and GLAST glutamate transporters are expressed on morphologically distinct astrocytes and regulated by neuronal activity in primary hippocampal cocultures.** *J Neurochem* 2000, **75**:1076–1084.
42. Gegelashvili G, Dehnes Y, Danbolt NC, Schousboe A: **The high-affinity glutamate transporters GLT1, GLAST, and EAAT4 are regulated via different signalling mechanisms.** *Neurochem Int* 2000, **37**:163–170.
43. Aronica E, Gorter JA, Ijlst-Keizers H, Rozemuller AJ, Yankaya B, Leenstra S, Troost D: **Expression and functional role of mGluR3 and mGluR5 in human astrocytes and glioma cells: opposite regulation of glutamate transporter proteins.** *Eur J Neurosci* 2003, **17**:2106–2118.
44. González-Mejia ME, Morales M, Hernández-Kelly LC, Zepeda RC, Bernabé A, Ortega A: **Glutamate-dependent translational regulation in cultured Bergmann glia cells: involvement of p70S6K.** *Neuroscience* 2006, **141**:1389–1398.
45. Zepeda RC, Barrera I, Castelán F, Suárez-Pozos E, Melgarejo Y, González-Mejia E, Hernández-Kelly LC, López-Bayghen E, Aguilera J, Ortega A: **Glutamate-dependent phosphorylation of the mammalian target of rapamycin (mTOR) in Bergmann glial cells.** *Neurochem Int* 2009, **55**:282–287.
46. Stanbrough M, Rowen DW, Magasanik B: **Role of the GATA factors Gln3p and Nil1p of Saccharomyces cerevisiae in the expression of nitrogen-regulated genes.** *Proc Natl Acad Sci USA* 1995, **92**:9450–9454.

doi:10.1186/1742-2094-9-275
Cite this article as: Takaki *et al.*: L-glutamate released from activated microglia downregulates astrocytic L-glutamate transporter expression in neuroinflammation: the 'collusion' hypothesis for increased extracellular L-glutamate concentration in neuroinflammation. *Journal of Neuroinflammation* 2012 **9**:275.

ACS Chemical Neuroscience

Research Article

pubs.acs.org/acschemicalneuroscience

Discovery of a Tamoxifen-Related Compound that Suppresses Glial L-Glutamate Transport Activity without Interaction with Estrogen Receptors

Kaoru Sato,*[,‡,†] Jun-ichi Kuriwaki,[‡,†] Kanako Takahashi,[‡] Yoshihiko Saito,[§] Jun-ichiro Oka,[§] Yuko Otani,[∥] Yu Sha,[∥] Ken Nakazawa,[‡] Yuko Sekino,[‡] and Tomohiko Ohwada*[,∥]

[‡]Laboratory of Neuropharmacology, Division of Pharmacology, National Institute of Health Sciences, 1-18-1 Kamiyoga, Setagaya-ku, Tokyo 158-8501, Japan

[§]Laboratory of Pharmacology, Faculty of Pharmaceutical Sciences, Tokyo University of Science, 2541 Yamazaki, Noda-city, Chiba 278-8510, Japan

[∥]Laboratory of Organic and Medicinal Chemistry, Graduate School of Pharmaceutical Sciences, University of Tokyo, 7-3-1, Hongo, Bunkyo-ku, Tokyo 113-0033, Japan

ABSTRACT: We recently found that tamoxifen suppresses L-glutamate transport activity of cultured astrocytes. Here, in an attempt to separate the L-glutamate transporter-inhibitory activity from the estrogen receptor-mediated genomic effects, we synthesized several compounds structurally related to tamoxifen. Among them, we identified two compounds, **1** (YAK01) and **3** (YAK037), which potently inhibited L-glutamate transporter activity. The inhibitory effect of **1** was found to be mediated through estrogen receptors and the mitogen-activated protein kinase (MAPK)/phosphatidylinositol 3-kinase (PI3K) pathway, though **1** showed greatly reduced transactivation activity compared with that of 17β-estradiol. On the other hand, compound **3** exerted its inhibitory effect through an estrogen receptor-independent and MAPK-independent, but PI3K-dependent pathway, and showed no transactivation activity. Compound **3** may represent a new platform for developing novel L-glutamate transporter inhibitors with higher brain transfer rates and reduced adverse effects.

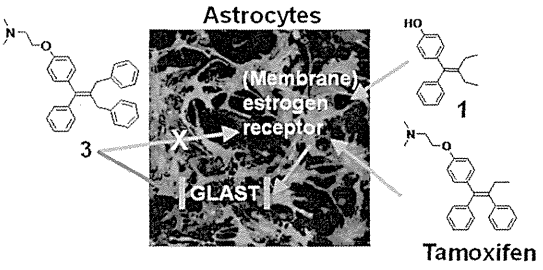

Inhibition of glial L-glutamate transporter

KEYWORDS: *Tamoxifen, astrocyte, L-glutamate transporter, ERα, tetrasubstituted ethylene, nongenomic pathway*

L-Glutamate (L-Glu) is one of the major excitatory neurotransmitters in the central nervous system (CNS), but high concentrations of extracellular L-Glu cause excessive stimulation of L-Glu receptors in the CNS, leading to neurotoxicity.[1,2] Astrocyte L-Glu transporters are the only machinery available to remove L-Glu from extracellular fluid and to maintain a low and nontoxic concentration of L-Glu.[3] Consequently, dysfunction of astrocyte L-Glu transporters is considered to be implicated in the pathology of neurodegenerative conditions.[4] Therefore, exogenous compounds that can regulate the function of L-Glu transporters may provide chemical tools to investigate the regulatory mechanisms of these transporters at the molecular level, and would also be candidate therapeutic agents.

There is growing evidence that estrogen receptor (ER) α, which is a nuclear ER (nER) that mediates genomic effects, can also be translocated to plasma membranes and mediate acute nongenomic effects in some cases. We have clarified that 17β-estradiol (E2) inhibits L-Glu transporters via a nongenomic pathway involving membrane-associated ERα (mERα).[5] Tamoxifen (Tam), a synthetic estrogen analogue that is clinically used in the treatment of breast cancer to block the proliferative action of estrogens,[6] also inhibited astrocyte L-Glu transporters at picomolar concentration, probably through the same nongenomic pathway as E2.[7] Because overexpression of astrocyte L-Glu transporters is often associated with neuropsychiatric disorders,[4] inhibitors of L-Glu transporters may be clinically useful to ameliorate these disorders.[8] However, Tam also acts on genomic pathways involving nuclear estrogen receptors (nERs) α and β, depending on the cell type and promoter context,[9] and so may cause adverse effects including endometrial changes, depression and weight gain.[10,11] Therefore, Tam-inspired compounds that retain the inhibitory effect on L-Glu transporters, but lack the nER-mediated genomic effects, would be useful tools for biological research, as well as candidate therapeutic agents.

Tam is a tetrasubstituted triphenylethylene derivative, in which the four substituents on the olefinic carbon atoms are different. This structural complexity makes the stereospecific synthesis of Tam-related derivatives difficult. We thus focused on Tam-inspired compounds bearing identical substituents on at least one of the olefinic carbon atoms.[12] It is well-known that the *N,N*-dimethylaminoethyl substituent on the phenolic oxygen atom and the regiochemistry of the tetrasubstituted

Received: September 29, 2011
Accepted: November 14, 2011
Published: November 14, 2011

olefin of Tam are crucial for ER binding activity.[13] So, we considered that more symmetrical derivatives of Tam might show reduced ER-binding ability.

Among our synthesized compounds, we found two, compounds **1** (YAK01) and **3** (YAK037), with potent L-Glu transporter-inhibitory activity. Studies of their mechanisms of action indicated that, unlike Tam, compound **3** acts through an ER-independent and MAPK-independent, but PI3K-dependent pathway and shows no transactivation activity for nERs. We believe this compound may represent a new platform for developing novel L-Glu transporter inhibitors with higher brain transfer rates and reduced adverse effects.

RESULTS AND DISCUSSION

We synthesized several Tam-inspired compounds bearing identical substituents on one carbon atom of the olefin,[12] and found that two of them were potent inhibitors of astrocyte L-Glu transporters. The diethyl-substituted derivative **1** inhibited L-Glu transporters in the picomolar range (62.7 ± 7.48% of control at 1 pM; Figure 2A). The dose–response curve for the inhibitory activity was not linear, but followed an inverted U-shaped curve; however, such a non-monotonic dose dependence is rather common for hormones and their mimetics.[14] On the other hand, when the symmetrical substituent was changed from ethyl to benzyl (**2**), the inhibitory effect was lost (Figure 2B). However, when the phenolic oxygen atom of **1** was substituted with a *N*,*N*-dimethylaminoethyl group (Figure 1C), we found

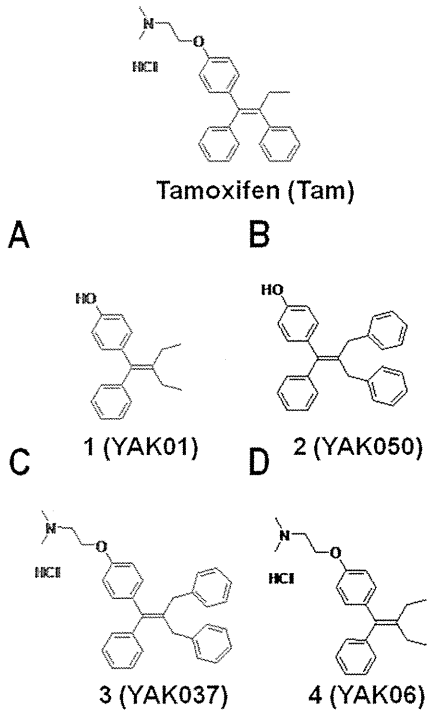

Figure 1. Chemical structures of the newly synthesized tamoxifen-related compounds.

that the resulting compound **3** showed dose-dependent L-Glu transporter inhibition in the picomolar range (63.8 ± 5.49% of control at 1 pM; Figure 2C). The dose-dependency of the effect of **3** suggested that the underlying mechanism might be different from that in the case of **1**. Compound **4** was inactive (Figure 2D).

We next examined the effects of **1** and **3** on cell viability by means of MTT reduction assay and LDH leakage assay, using the same cultured sample. Neither of the compounds was cytotoxic at concentrations below 1 μM (Figure 3), though 100 μM **1** and 10 μM **3** caused severe cell damage. These results exclude the possibility that the L-Glu clearance-inhibitory effects of these compounds at concentrations below 1 μM were caused by cell damage.

In order to confirm the involvement of L-Glu transporters in the inhibition of L-Glu uptake by our compounds, and to rule out the possibility that **1** and **3** act by inducing L-Glu release from astrocytes, we next examined the effect of **1** and **3** on L-Glu clearance when the L-Glu transporter activity was blocked with TBOA, a potent nonselective L-Glu transporter inhibitor (IC_{50}: 48 μM for GLAST/EAAT1, 7 μM for GLT1/EAAT2). We confirmed that application of 1 mM TBOA potently inhibited L-Glu transporter activity; that is, TBOA caused reversible chemical knock-down of L-Glu transporter activity.[7] When either **1** or **3** was coapplied with 1 mM TBOA, these compounds no longer influenced L-Glu clearance (Figure 4), indicating that the actions of these compounds are indeed mediated by L-Glu transporters, and do not involve L-Glu release from astrocytes.

Our cultured astrocytes predominantly expressed ERα, and little or no expression of ERβ was detected.[5] Tam is known to be a partial agonist of ERs,[9] raising the possibility that the compounds exerted their inhibitory effects via interaction with ERα. Therefore, we examined the involvement of ERα by coapplication of ICI182,780, a high-affinity antagonist of ERs. ICI182,780 dose-dependently blocked the inhibition of L-Glu uptake caused by **1** (Figure 5A) at 0.01, 0.1, and 1 μM, at which the effects of Tam were reported to be completely suppressed.[7] In contrast, ICI182,780 had no effect on the inhibition by **3** (Figure 5B), suggesting that the mechanism of the inhibition by **3** is independent of ERs. We further examined the signal transduction pathways mediating the effects of **1** and **3**. When coapplied with U0126, which inhibits mitogen-activated protein kinase/extracellular signal-regulated kinase 1 (MEK1, IC50: 70 nM) and MEK2 (IC50: 60 nM), the inhibitory effect by **1** was blocked, whereas that of **3** was not (Figure 6A). On the other hand, when coapplied with LY294002, a specific phosphoinositide 3-kinase (PI3K) inhibitor (IC50: 70 nM), the inhibitory effects of both compounds were completely blocked (Figure 6B). These results suggest that PI3K is a common mediator of the effects of both compounds, whereas mitogen-activated protein kinase (MAPK) is involved only in the mechanism of inhibition by **1**.

Finally we examined the ER-agonist potency of **1** and **3**, i.e., the transcriptional effects of these compounds via human ERα and ERβ, using HEK293/hERα and HEK293/hERβ reporter cells (Figure 7). Compound **1** showed agonist activity in both of 293/hERα and 293/hERβ reporter cells, though the binding affinities were much weaker than that of E2. The EC50 values of **1** for ERα and ERβ are 30.8 nM and 10.4 nM, respectively (1.25 nM and 0.864 nM, respectively, for E2). The relative agonist activity of **1** was 66.8% of that of E2 in HEK293/hERα and 122.0% of that of E2 in HEK293/hERβ. Strikingly, **3** showed no agonist potency for ERα or ERβ. These findings strongly suggest that **3** can inhibit L-Glu transporters without interaction with ERs.

In this study, we examined the potential of Tam-related compounds to inhibit GLAST/EAAT1 and GLT1/EAAT2, which are major astrocytic L-Glu transporters in the rat

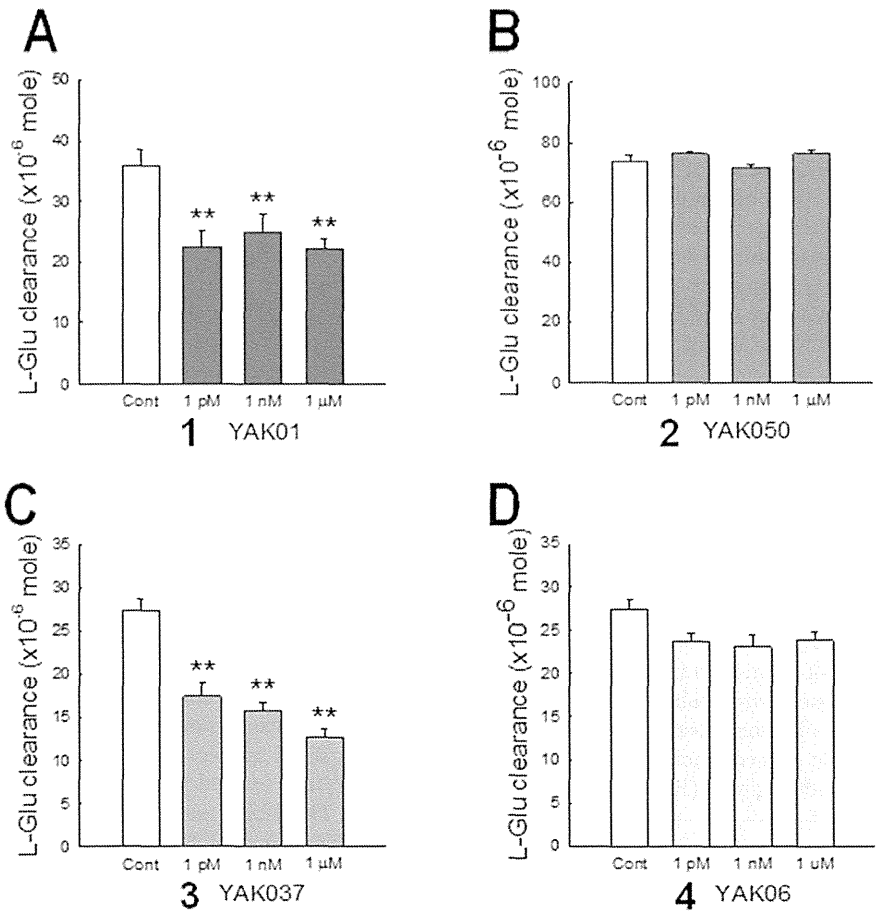

Figure 2. Compounds **1** and **3** inhibited L-Glu clearance in cultured astrocytes. The open column shows the control clearance, and colored columns show the clearance in the presence of various concentrations of compounds **1** (A), **2** (B), **3** (C), and **4** (D). $^{**}p < 0.01$ vs control group ($N = 6$), Tukey's test following ANOVA.

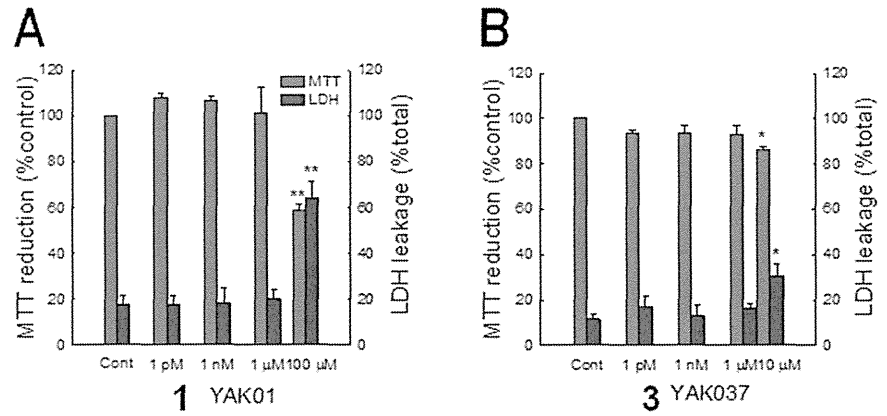

Figure 3. Effects of compounds **1** and **3** on cell viability. The results of MTT reduction and LDH leakage assays of **1** (A) and **3** (B) are shown. $^{*}p < 0.05$, $^{**}p < 0.01$ vs control group ($N = 6$), Tukey's test following ANOVA.

forebrain. Although GLT-1 is the main regulator of synaptically released L-Glu in vivo, the predominant subtype changes to GLAST in cultured astrocytes, possibly owing to the lack of interaction of astrocytes with neurons.[15] We confirmed that GLAST is the main functional L-Glu transporter in our primary-cultured astrocytes by Western blotting and pharmacological experiments (data not shown), in accordance with a previous report.[16] Therefore, the effects of the compounds observed here can be interpreted as being due to modulation of GLAST functional activity.

There is growing evidence that ERα, which is a nER that mediates genomic effects, can also be translocated to plasma membranes and mediate acute nongenomic effects in some cases. Transfection of CHO cells with nERs was reported to result in ER expression in both nuclei and membranes.[17] ERs on the plasma membranes of tumor cells were demonstrated to be structurally similar to nERs.[18] Further, mERα activated metabotropic glutamate receptor 5 (mGluR5) in striatal neurons in the CNS.[19] In our previous study, we clarified that the predominant ER subtype in cultured astrocytes was ERα, and

dx.doi.org/10.1021/cn200091w | ACS Chem. Neurosci. 2012, 3, 105–113

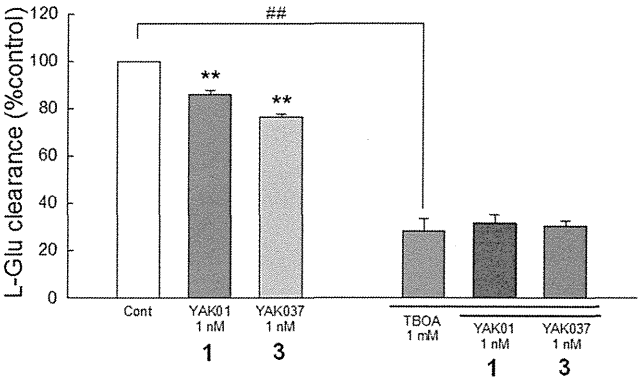

Figure 4. Compounds **1** and **3** suppressed L-Glu clearance in astrocyte culture by decreasing the functional activity of L-Glu transporter. L-Glu clearance in the presence and absence of compounds **1** and **3** is shown, together with their effects in the copresence of the potent nonselective L-Glu transporter inhibitor TBOA. $^{**}p < 0.01$ vs control group ($N = 6$), Tukey's test following ANOVA.

estrogens (such as E2 and Tam) inhibited L-Glu transporter activity via the activation of mERα.[5] We found that the effects of **1** were blocked by ICI182,780, suggesting an interaction of **1** with ERα. In addition, our pharmacological experiments showed that activation of both of MAPK and PI3K is necessary for the L-Glu transporter-inhibitory activity of **1**. There are many reports indicating that nongenomic effects involving mERα are mediated via MAPK[19−21] and PI3K.[20,22] Taken together, the effects of **1** may be mediated by mERα in a similar manner to E2 and Tam. E2 was reported to activate MAPK via both PI3K-dependent and independent pathways in a single neuron.[20] Whether or not the same signaling pathways also exist in astrocytes is not yet known. It is of interest that other studies have found that estrogens also inhibit dopamine transporter (DAT) through the activation of mERα.[23,24]

On the other hand, the effect of **3** was ER-independent and MAPK-independent, but PI3K-dependent. Our binding assay revealed that **1** binds with ERs, but **3** does not. Based on these results, we propose that the mechanisms of the L-Glu

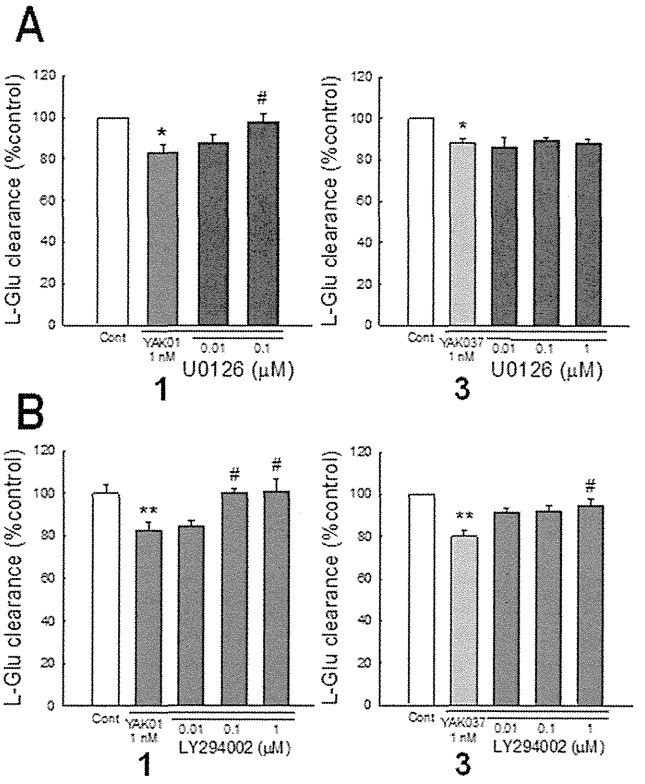

Figure 6. Involvement of MAPK and PI3K in the L-Glu transporter-inhibitory activity of compounds **1** (A) and **3** (B). Effects of compounds **1** (left panels) and **3** (right panels) on L-Glu clearance in the presence and absence of various concentrations of U0126, an inhibitor of MAPK/ERKs (A) or LY294002, a specific inhibitor of PI3K (B). $^{*}P < 0.05$, $^{**}p < 0.01$ vs control group, $\#p < 0.05$ vs compound-treated group ($N = 6$), Tukey's test following ANOVA.

transporter-inhibitory effects of **1** and **3** are different, as illustrated in Figure 8. The effect of **3** was possibly mediated by GPR30, a newly found ER, which is suggested to mediate the rapid nongenomic effects of estrogens.[25,26] In the case of GPR30, ICI182,780 acts as agonist, leading to activation of

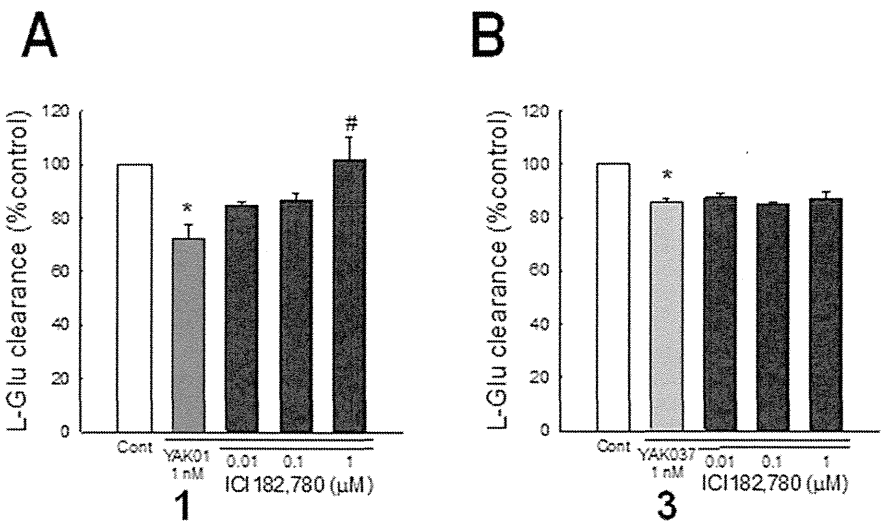

Figure 5. Involvement of ERs in the L-Glu transporter-inhibitory effects of compounds **1** and **3**. Effects of compounds **1** (A) and **3** (B) on L-Glu clearance in the presence and absence of various concentrations of ICI182,780, a high-affinity antagonist of ERs. $^{*}P < 0.05$ vs control group, $\#p < 0.05$ vs compound-treated group ($N = 6$), Tukey's test following ANOVA.

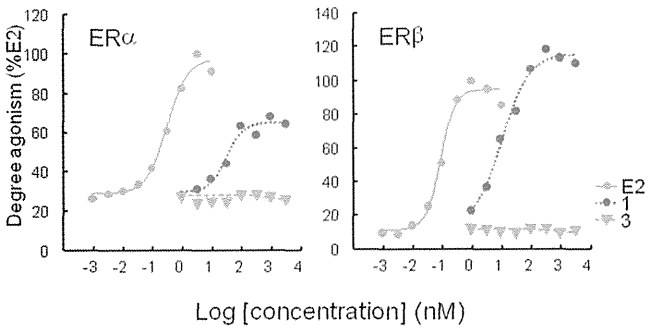

Figure 7. ER agonist potency of compounds **1** and **3** to nERs: dose dependence of binding of compounds **1** and **3** in HEK293/hERα cells (left) or HEK293/hERβ cells (right). Compound 1 showed dose-dependent agonist activity in both of HEK293/hERα cells (left) and HEK293/hERβ cells (right), though 3 showed no agonist potency for ERα or ERβ.

signal transduction pathways in a similar manner to estrogens.[27,28] However, we could not detect any effects of ICI182,780 alone on L-Glu transporter in our experiments (data not shown). In addition, Kuo et al. reported that GPR30 in astrocytes is detected not in the cell membranes but in the smooth endoplasmic reticulum,[29] while the cellular localization of GPR30 has been still controversially argued. In these contexts, GPR30 is an unlikely mediator to block the L-Glu transporters by the action of **3**.

According to Kisanga et al., the concentration of Tam in serum during conventional treatment for breast cancer (1–20 mg daily) is in the range from 20 to 225 nM.[30] Because **3** is more hydrophobic than Tam (the values of clogP for Tam and **3** are 7.56 and 9.70, respectively), it should exhibit greater permeability into the brain. Although other L-Glu transporter inhibitors, mainly L-Glu/aspartate analogues, are known, few of them have high brain transfer rates. Therefore, **3** is expected to be useful for biological research, and is also considered to be a promising candidate or lead compound for pharmacological application.

In conclusion, examination of several Tam-inspired compounds led to the discovery of two compounds that inhibited astrocytic L-Glu transporters at picomolar concentration. The inhibitory activity of compound **1** was mediated through the ER-MAPK/PI3K pathway, like that of Tam, though its transactivation activity was drastically reduced as compared with E2. In contrast, the inhibitory effect of **3** was manifested through an ER-independent and MAPK-independent, but PI3K-dependent pathway, and **3** showed no transactivation activity. These results suggest that **3** may represent a new platform for the development of novel L-Glu transporter inhibitors with higher brain transfer rates and reduced adverse effects.

METHODS

Chemistry. *General Procedures.* All reagents were commercial products and were used without further purification, unless otherwise noted. NMR data were recorded on a JEOL-400 or a Bruker Avance 400 NMR spectrometer (400 MHz for ^{1}H NMR and 100 MHz for ^{13}C NMR). *d*-$CDCl_3$ was used as a solvent, unless otherwise noted. Chemical shifts (δ) are reported in ppm with respect to internal tetramethylsilane (δ = 0 ppm) or undeuterated residual solvent (i.e., $CHCl_3$ (δ = 7.265 ppm)). Coupling constants are given in hertz. Coupling patterns are indicated as follows: m = multiplet, d = doublet, s = singlet, br = broad. High-resolution mass spectrometry (HRMS) was conducted in the electron spray ionization (ESI)-time-of-flight

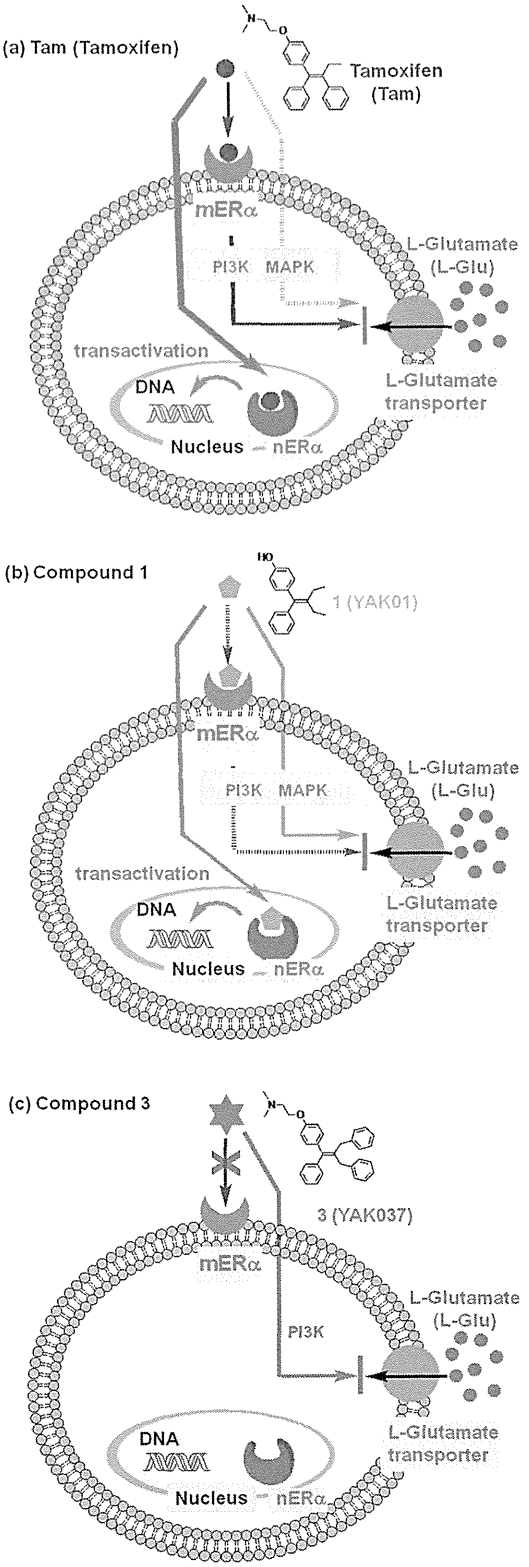

Figure 8. Schematic illustration of the proposed mechanisms of the effects of tamoxifen (a) and compounds **1** (b) and **3** (c).

(TOF) detection mode on a Bruker micrOTOF-05. FAB-MS and high-resolution FAB-MS were obtained on a JMS700-MSTATION (JEOL, Japan). Column chromatography was carried out on silica gel (silica gel 60N (100–210 μm), Kanto Chemicals, Japan). Flash column chromatography was performed on silica gel H (Merck, Germany). Analytical thin-layer chromatography (TLC) was performed on

dx.doi.org/10.1021/cn200091w | ACS Chem. Neurosci. 2012, 3, 105–113

precoated plates of silica gel HF_{254} (Merck, Germany). All the melting points were measured with a Yanaco Micro Melting Point apparatus and are uncorrected. Combustion analyses were carried out in the microanalysis laboratory of this faculty.

Synthesis of Compounds. Compounds **1** and **2** were synthesized from 4-hydroxybenzophenone and butyl-3-one or dibenzylacetone by using $TiCl_4$ in the presence of Zn. Introduction of the *N,N*-dimethylaminoethyl moiety at the phenolic hydroxyl group of **1** and **2** was carried out by base treatment, followed by addition of 2-dimethylaminoethyl chloride hydrochloride.

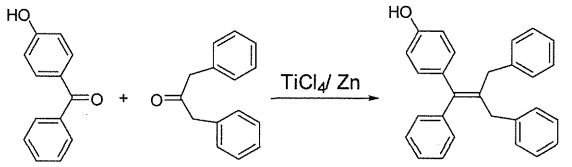

2 (YAK050)

Synthesis of Tamoxifen-Related Compounds. Compound 2 (YAK050). To a suspension of Zn powder (916.6 mg; 6.9 equiv with respect to 4-hydroxybenzophenone) in dry THF (30 mL) in a 200 mL three-necked flask, $TiCl_4$ (0.61 mL, 2.8 equiv) was added dropwise under an argon atmosphere at −20 °C (in an ice-salt bath) over 2 min. The resulting light green-yellow mixture was stirred at −20 °C for 20 min and then the cooling bath was removed. After 20 min, the flask was immersed in a preheated oil bath at 100 °C and refluxed at 100 °C with stirring for 2.5 h. To the resulting deep blue mixture was added in one portion a solution of 4-hydroxybenzophenone (401.3 mg, 2.02 mmol) and dibenzyl ketone (1.2735 g, 3 equiv) in 50 mL of dry THF. The resultant mixture was heated at reflux at 100 °C with stirring for 2 h, then allowed to cool to rt, and poured into 400 mL of 0.5 N aqueous NaOH solution. The whole was extracted with ethyl acetate (500 mL). The organic layer was washed with water, dried over $MgSO_4$ and evaporated to give a pale yellow oil (1.5172 g), which was column-chromatographed (silica gel, acetone/*n*-hexane (1:7)) to give 365.0 mg (48% yield) of the olefin **2** as a white amorphous solid. Mp: 57–60 °C. ^1H NMR ($CDCl_3$): δ: 7.287–7.079 (m, 17H), 6.760 (d, 2H, J = 8.8 Hz), 4.792 (s, 1H), 3.413 (s, 2H), 3.377 (s, 2H). ^{13}C NMR ($CDCl_3$): δ: 154.1, 143.0, 140.7, 140.4, 135.8, 135.4, 130.7, 129.4, 128.8, 128.3, 128.3, 128.2, 126.5, 125.9, 115.1, 37.4, 37.2. HRMS (ESI^-): Calcd. for $C_{28}H_{23}O$ ($[M - H]^-$), 375.1754. Found: 375.1744. Anal. Calcd for $C_{28}H_{24}O{\cdot}0.2H_2O$: C, 88.48; H, 6.47; N, 0.00. Found: C, 88.36; H, 6.63; N, 0.00.

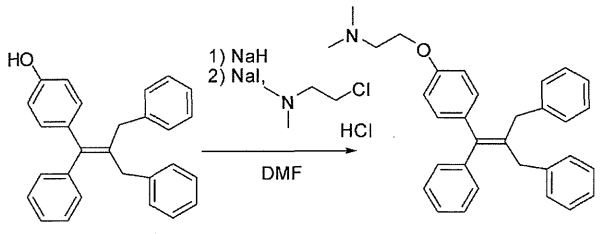

2 (YAK050)

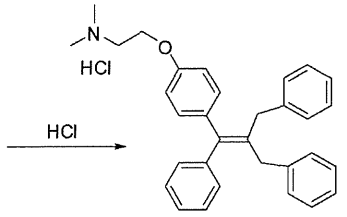

3 (YAK037)

Compound 3 (YAK037). To a suspension of NaH (60%, 42 mg, 1.05 mmol) in DMF (3 mL) at 0 °C was added a solution of the phenol **2** (158.2 mg, 0.420 mmol) in DMF (3 mL). The reaction mixture was stirred for 30 min at 0 °C, and then a solution of 2-dimethylaminoethyl chloride hydrochloride (181.0 mg, 1.256 mmol, 3.0 equiv) and NaI (94.0 mg, 0.627 mmol, 1.5 equiv) in DMF (3 mL) was added. The reaction mixture was stirred at 50 °C for 30 min, and then saturated aqueous NH_4Cl was added to quench the reaction. The mixture was extracted with Et_2O. The organic layer was washed with brine, dried over Na_2SO_4 and evaporated to afford a residue, which was column-chromatographed (ethyl acetate/Et_3N = 100/1) to give the intermediate amine (83.0 mg, 44% yield). The HCl salt of the resultant amine was prepared by repeated addition of a solution of 2 N HCl in Et_2O to a solution of the amine in ethyl acetate, followed by evaporation of the organic solvent to give **3**.

3: White solid. Mp. 169–170 °C. ^1H NMR ($CDCl_3$): δ: 13.073 (brs, 1H), 7.306–7.195 (m, 13H), 7.102–7.074 (m, 4H), 6.832 (d, 2H, J = 8.8 Hz), 4.481–4.459 (m, 2H), 3.425–3.390 (m, 6H), 2.893 (s, 6H). ^{13}C NMR ($CDCl_3$) δ: 155.7, 142.8, 140.4, 140.3, 140.2, 136.8, 136.2, 130.9, 129.4, 128.8, 128.7, 128.4, 128.3, 128.3, 126.6, 126.0, 125.9, 114.3, 62.8, 56.5, 43.6, 37.4, 37.2. HRMS (ESI^+, $[M + H]^+$): Calcd. for $C_{32}H_{34}NO$, 448.26349. Found: 448.26092. Anal. Calcd for $C_{32}H_{34}ClNO{\cdot}1/4H_2O$: C, 78.67; H, 7.12; N, 2.87. Found: C, 78.64; H, 7.30; N, 2.87.

Compound 1 (YAK01).

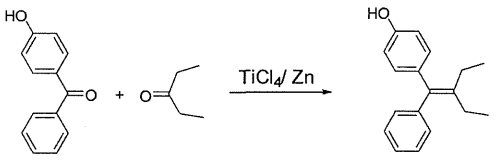

1 (YAK01)

To a suspension of Zn (0.86 g, 13.2 mmol) in 30 mL of dry THF at −5 °C was added dropwise $TiCl_4$ (0.72 mL, 6.6 mmol) under an argon atmosphere. The mixture was heated at reflux for 2 h. A solution of 4-hydroxybenzophenone (341.1 mg, 1.7 mmol) and 3-pentanone (0.50 mL, 5.0 mmol) in 50 mL of dry THF was added in one portion, and heating was continued at reflux for 6 h. Then the reaction mixture was cooled to rt, quenched with 10% aqueous K_2CO_3 (100 mL) and extracted with ethyl acetate (3 × 80 mL). The combined organic phase was washed with brine (50 mL), dried over Na_2SO_4, and evaporated to give a residue, which was flash column-chromatographed (3:1 hexane/ethyl acetate) to afford **1** (383.4 mg, 88.3%) as a white solid.

1: Mp. 76.0–76.5 °C (colorless needles, recrystallized from *n*-hexane). ^1H NMR ($CDCl_3$) δ: 7.261 (2H, t, J = 8.0 Hz), 7.173 (1H, d, J = 7.2 Hz), 7.128 (2H, d, J = 7.6 Hz), 7.009 (2H, d, J = 8.8 Hz), 6.726 (2H, d, J = 8.8 Hz), 4.763 (1H, s), 2.152 (2H, quartet, J = 7.6 Hz), 2.115 (2H, quartet, J = 6.0 Hz), 1.007 (3H, t, J = 7.6 Hz), 0.994 (3H, t, J = 7.6 Hz). ^{13}C NMR ($CDCl_3$) δ: 153.7, 143.7, 142.0, 136.5, 136.2, 130.5, 129.2, 127.9, 125.9, 114.8, 24.4, 24.3, 13.3. HRMS (ESI^-, $[M - H]^-$): Calcd. for $C_{18}H_{19}O^-$, 251.14414. Found: 251.14730. HRMS (FAB-MS, $[M]^+$) Calcd. for $C_{18}H_{20}O$, 252.1514. Found: 252.1528. Anal. Calcd. for $C_{18}H_{20}O$: C, 85.67; H, 7.99; N, 0.00. Found: C, 85.38; H, 8.13; N, 0.00.

Compound 4 (YAK06).

2-Dimethylaminoethyl chloride hydrochloride (282.4 mg, 2.0 mmol) and K_2CO_3 (1.5734 g, 11.4 mmol) were stirred in acetone/H_2O (18 mL/2 mL) at 0 °C for 30 min, then compound **1** (139.1 mg, 0.55 mmol) and K_2CO_3 (421.1 mg, 3.1 mmol) were added, and the whole was heated at reflux for 24 h, then cooled to rt. Inorganic materials were removed by filtration, and the filtrate was evaporated. The residue was flash column-chromatographed (100:1 ethyl acetate/Et_3N) to afford the amine as a white solid (88.0 mg). To a solution of the amine in ethyl acetate, a solution of HCl in ether was added to give a precipitate, which was collected and recrystallized from ethanol/ethyl acetate to give **4** (95.0 mg, 48%) as a white powder. **4**: Mp. 129.5–130.2 °C. ^1H NMR ($CDCl_3$) δ 726–6.90 (9H, m), 4.07 (2H, t, J = 6.0 Hz), 2.75 (2H, t, J = 6.0 Hz), 2.40 (6H, s), 2.15 (4H, d, J = 7.2 Hz), 1.00 (6H, t, J = 7.2 Hz). HRMS (FAB-MS, $[M\text{-}Cl]^+$): Calcd. for $C_{22}H_{30}NO^+$: 324.2322. Found: 324.2321.